

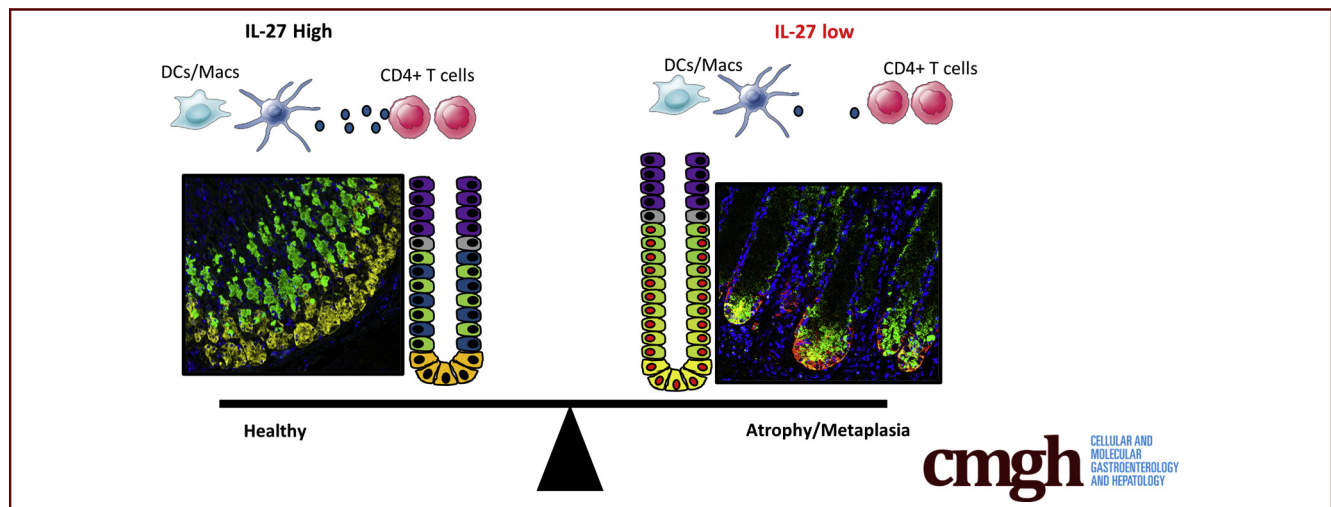
ORIGINAL RESEARCH

Interleukin 27 Protects From Gastric Atrophy and Metaplasia During Chronic Autoimmune Gastritis



Kevin A. Bockerstett,¹ Christine P. Petersen,³ Christine N. Noto,¹ Lindsey M. Kuehm,¹ Chun Fung Wong,¹ Eric L. Ford,¹ Ryan M. Teague,¹ Jason C. Mills,² James R. Goldenring,³ and Richard J. DiPaolo¹

¹Department of Molecular Microbiology and Immunology, Saint Louis University School of Medicine, Saint Louis, Missouri; ²Division of Gastroenterology, Department of Medicine, Pathology and Immunology, Department of Developmental Biology, Washington University School of Medicine, Saint Louis, Missouri; and ³Nashville Veterans Affairs Medical Center, Department of Surgery, Department of Cell and Developmental Biology, Epithelial Biology Center, Vanderbilt University School of Medicine, Nashville, Tennessee



SUMMARY

Interleukin (IL27) suppresses atrophy and metaplasia during chronic autoimmune gastritis. Mice lacking IL27 rapidly develop atrophy and metaplasia whereas mice treated with IL27 are protected from disease as a result of the effect of this cytokine on CD4 T cells.

BACKGROUND & AIMS: The association between chronic inflammation and gastric carcinogenesis is well established, but it is not clear how immune cells and cytokines regulate this process. We investigated the role of interleukin 27 (IL27) in the development of gastric atrophy, hyperplasia, and metaplasia (preneoplastic lesions associated with inflammation-induced gastric cancer) in mice with autoimmune gastritis.

METHODS: We performed studies with TxA23 mice (control mice), which express a T-cell receptor against the H+/K+ adenosine triphosphatase α chain and develop autoimmune gastritis, and TxA23x*Ebi3*^{-/-} mice, which develop gastritis but do not express IL27. In some experiments, mice were given high-dose tamoxifen to induce parietal cell atrophy and spasmodic polypeptide-expressing metaplasia (SPEM).

Recombinant IL27 was administered to mice with mini osmotic pumps. Stomachs were collected and analyzed by histopathology and immunofluorescence; we used flow cytometry to measure IL27 and identify immune cells that secrete IL27 in the gastric mucosa. Single-cell RNA sequencing was performed on immune cells that infiltrated stomach tissues.

RESULTS: We identified IL27-secreting macrophages and dendritic cell in the corpus of mice with chronic gastritis (TxA23 mice). Mice deficient in IL27 developed more severe gastritis, atrophy, and SPEM than control mice. Administration of recombinant IL27 significantly reduced the severity of inflammation, atrophy, and SPEM in mice with gastritis. Single-cell RNA sequencing showed that IL27 acted almost exclusively on stomach-infiltrating CD4+ T cells to suppress expression of inflammatory genes.

CONCLUSIONS: In studies of mice with autoimmune gastritis, we found that IL27 is an inhibitor of gastritis and SPEM, suppressing CD4+ T-cell-mediated inflammation in the gastric mucosa. (*Cell Mol Gastroenterol Hepatol* 2020;10:561–579; <https://doi.org/10.1016/j.jcmgh.2020.04.014>)

Keywords: Mouse Model; Immune Regulation; Lymphocyte; Transcription.

Chronic inflammation is a driving factor in several gastrointestinal disease processes, including gastric cancer.¹ Gastric cancer is the sixth most common and the third most deadly cancer in the world, representing a significant global health issue.² This is in part because gastritis is relatively common, primarily because of the high prevalence of *Helicobacter pylori* infections, but also other etiologies such as autoimmunity.^{3,4} Although adenocarcinoma is associated most commonly with *Helicobacter* infection, a recent study of patients with autoimmune gastritis-induced metaplasia showed that these patients also have a significantly higher rate of adenocarcinoma relative to the general population.⁵ Furthermore, although overall gastric cancer decreased in the United States between 1995 and 2003, noncardia gastric adenocarcinoma is increasing. The increase of gastric cancer was attributed specifically in the gastric corpus and disproportionately impacts young women (age, <50 y).⁶ The decrease in *H pylori* infections in the United States has led to speculation that this new gastric cancer could be related to autoimmunity, which would explain the predilection of this novel gastric cancer for younger women. If this trend of increasing gastric adenocarcinoma continues, it potentially could result in an increase in overall gastric cancer cases.⁷

Host factors, such as cytokines produced by the inflammatory response, influence the development of gastric pathology and preneoplastic epithelial cell changes.⁸ This indicates that the phenotype of an individual's immune response during autoimmunity likely influences their risk of developing gastric cancer. Identifying cancer-promoting and -inhibiting components of the immune response is expected to provide significant diagnostic and therapeutic advances for patient care. In these studies, we used a mouse model of autoimmune gastritis to identify an important role for a cytokine (interleukin [IL]27), that suppresses CD4 T-cell-mediated inflammation in the gastric mucosa, thereby reducing the degree of atrophy and metaplasia during gastritis.


The development of gastric cancer is associated with a series of pathologic events in which chronic gastritis causes the loss of parietal and mature chief cells (atrophy), the development of mucous neck cell hyperplasia, spasmolytic polypeptide-expressing metaplasia (SPEM), intestinal metaplasia, dysplasia, and, eventually, adenocarcinoma.^{9,10} In recent years, there has been a focus on understanding SPEM, which often arises concomitantly with parietal and chief cell atrophy in a setting of chronic inflammation, because it may be a critical precursor for the development of intestinal metaplasia and adenocarcinoma.^{11,12} Although the loss of parietal and chief cells is associated strongly with the progression to metaplasia and carcinogenesis in this paradigm, parietal cell deletion, in the absence of inflammation, is not sufficient to induce metaplasia.¹³ In addition, recent data indicate that the phenotype of the inflammatory response is a critical determinant of SPEM development and progression.^{14,15} Therefore, inflammation not only promotes SPEM by damaging the epithelium and causing atrophy, it also may influence the severity and phenotype of SPEM by directly regulating metaplastic responses. We previously determined that cytokines (interferon [IFN] γ and IL17A)

secreted by immune cells can regulate the development of atrophy and SPEM by acting directly on epithelial cells.^{16,17} Elucidating the mechanism(s) by which cytokines either promote or prevent preneoplastic epithelial cell changes will improve the understanding of the pathophysiology of gastric carcinogenesis.

IL27 is a heterodimeric cytokine composed of 2 non-covalently associated proteins: p28 (encoded by the *Il27* gene) and EB13 (encoded by the *Ebi3* gene). The p28-Epstein-Barr Virus-Induced Gene (EB13) heterodimeric cytokine binds to the IL27 receptor, a heterodimer composed of IL27 receptor A (IL27RA) and gp130. IL27 receptors can be expressed on multiple cell types, including CD4 T cells. IL27 signals into T cells to promote the development of IFN γ -producing Th1 cells, and prevents the development of IL4-/IL13-producing T helper (Th)2 cells and IL17A-producing Th17 cells.^{18,19} IL27 is pleiotropic and has both proinflammatory and anti-inflammatory effects on many immune cells aside from CD4 Th cells (depending on the disease process and cell type acted upon).²⁰⁻²³ This cytokine has not been well studied in the context of autoimmune gastritis and gastric carcinogenesis, but the fact that IL27 regulates IFN γ and IL17A suggests a potentially critical role during gastritis because both of these cytokines act directly on gastric epithelium to promote parietal cell atrophy.^{16,17} Furthermore, it recently was determined that IL27 is highly expressed during *H pylori* infection in human patients.²⁴ In addition, IL27 plays a critical role in regulating the severity of disease in multiple mouse models of autoimmunity in various organ systems.^{25,26} This suggested that IL27 may play a role in regulating autoimmune gastritis. Studies of IL27 are complicated by the fact that the EB13 subunit of the heterodimer also might pair with p35 protein to form IL35, a poorly understood cytokine thought to be produced by regulatory T cells to inhibit T-cell proliferation.²⁷ Despite this possibility, recent studies have shown that IL27 specifically, and not IL35, ameliorates disease severity in several of these autoimmune conditions.²⁸⁻³⁰ In the context of these previous studies, we sought to determine the role of IL27 in the progression of gastritis toward gastric cancer, specifically in the development of key preneoplastic lesions, including atrophy and SPEM.

Here, we determined that IL27 was made in the mucosa by macrophages and dendritic cells during chronic gastritis.

Abbreviations used in this paper: APC, antigen-presenting cell; cDNA, complementary DNA; CD44v9, CD44 variant 9; EB1, Epstein-Barr Virus-Induced Gene; EpCAM, epithelial cell adhesion molecule; GIF, gastric intrinsic factor; GS-II, *griffonia simplicifolia*; HDT, high-dose tamoxifen; IF, immunofluorescent; IFN, interferon; IL, interleukin; MHC, major histocompatibility complex; PBS, phosphate-buffered saline; PDX1, pancreatic and duodenal homeobox 1; qRT-PCR, quantitative reverse-transcription polymerase chain reaction; rIL27, recombinant interleukin 27; scRNA, single-cell RNA; SPEM, spasmolytic polypeptide-expressing metaplasia; Th, helper T cell; Treg, regulatory T cells.

 Most current article

© 2020 The Authors. Published by Elsevier Inc. on behalf of the AGA Institute. This is an open access article under the CC BY-NC-ND license (<http://creativecommons.org/licenses/by-nc-nd/4.0/>).

2352-345X

<https://doi.org/10.1016/j.jcmgh.2020.04.014>

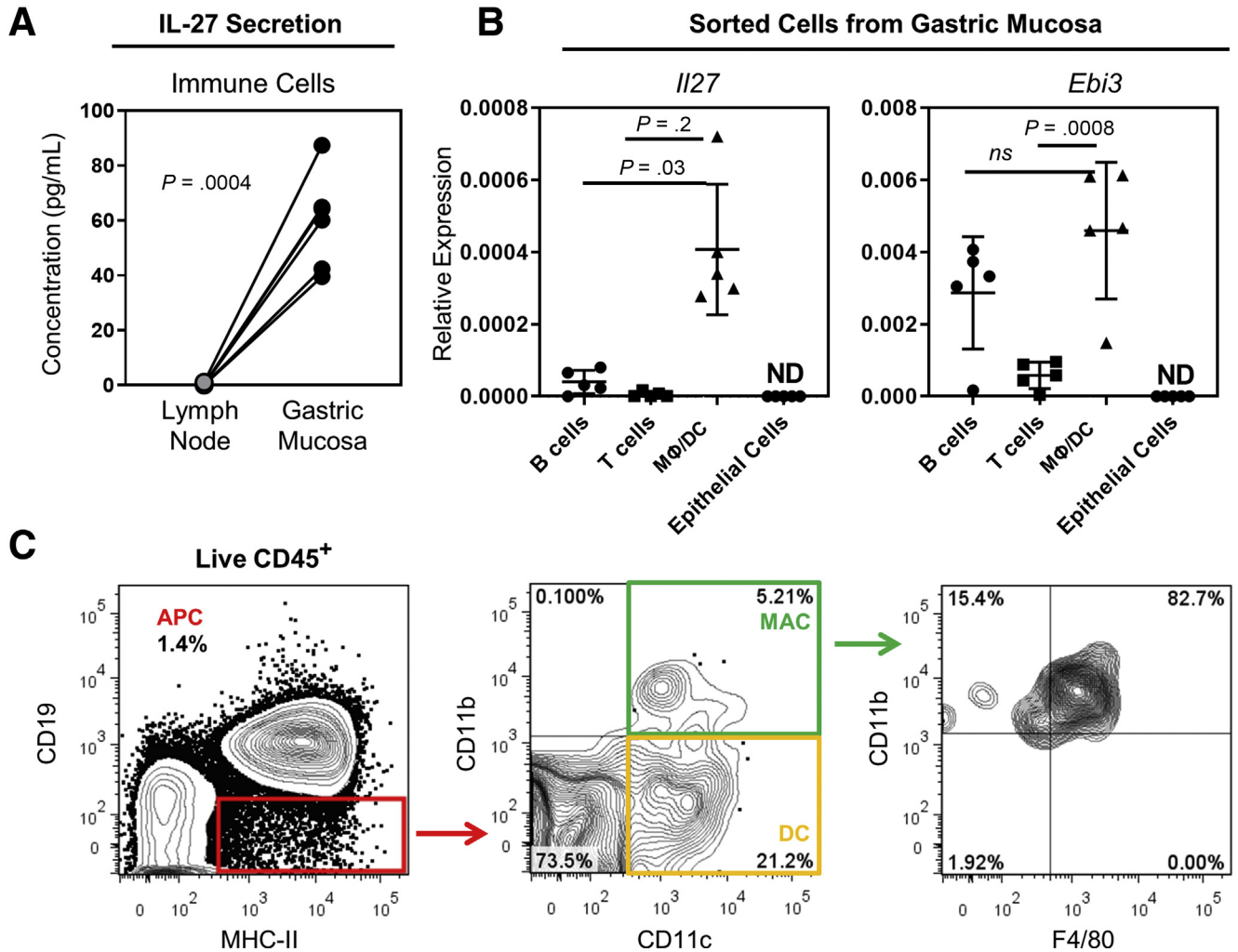


Figure 1. IL27 is secreted by macrophages/dendritic cells (DCs) in the gastric mucosa. (A) IL27 secretion measured by enzyme-linked immunosorbent assay from gastric lymph node cells (grey) or gastric mucosal immune cells (black) of TxA23 mice at 2 months of age. Each dot represents the data from 1 mouse, and samples from the same mouse are connected by a line. $N = 5$ mice per group from 2 separate experiments. Significance was determined using a Student t test. (B) Quantitative real-time PCR gene expression analysis for the 2 subunits of IL27 (*Il27* and *Ebi3*) in sorted and stimulated immune and epithelial cells isolated from the gastric mucosa. Expression of target genes was relative to the *Gapdh* housekeeping gene. Statistical significance was determined using a Student t test. $N = 3-5$ mice per group from 3 separate experiments. (C) Representative flow cytometry plots showing the gating strategy for identifying the presence of macrophages ($CD19^+MHCII^+CD11b^+CD11c^+F4/80^+$) and DCs ($CD19^+MHCII^+CD11b^+CD11c^+$) in the APC compartment of immune cells flushed from the gastric mucosa. ND, not determined.

To determine the role of IL27 during gastritis, *Ebi3*^{-/-} mice, which are unable to produce IL27 and IL35, were crossed onto a model of chronic autoimmune gastritis, TxA23. TxA23 mice express a transgenic T-cell receptor that is specific for a peptide from the H⁺/K⁺ adenosine triphosphatase α chain expressed by parietal cells. Autoreactive CD4⁺ T cells induce chronic autoimmune gastritis spontaneously early in life. Atrophy and metaplasia develop in the corpus of TxA23 mice, and similar to human beings with autoimmune gastritis, the antrum is spared.³¹ TxA23 mice mimic the disease progression observed in the corpus of human patients, including gastritis that progresses to atrophic gastritis with mucinous hyperplasia/metaplasia, development of SPEM, and, eventually, gastric

intraepithelial neoplasia.³² TxA23x*Ebi3*^{-/-} mice developed much more rapid and severe inflammation and atrophy as well as more extensive and proliferative SPEM throughout the entirety of the gastric corpus compared with control TxA23 mice. Studies using acute chemical parietal cell ablation showed that *Ebi3* was dispensable for SPEM development in response to acute damage, indicating IL27 specifically regulates inflammation-induced atrophy and metaplasia. Recombinant IL27 (rIL27) treatment prevented mice from developing gastritis-induced atrophy and SPEM, confirming that IL27 protects the stomach during chronic inflammation. Single-cell RNA (scRNA) sequencing analyses determined that IL27 specifically suppressed tissue-infiltrating effector CD4 T cells to reduce proinflammatory

transcripts. Together, these findings show that IL27 production is critical for suppressing CD4 T cells during chronic gastritis. In addition, they indicate that IL27 secretion in the gastric mucosa plays an important role in preventing the progression of gastritis to atrophy and metaplasia, critical steps in gastric cancer development.

Results

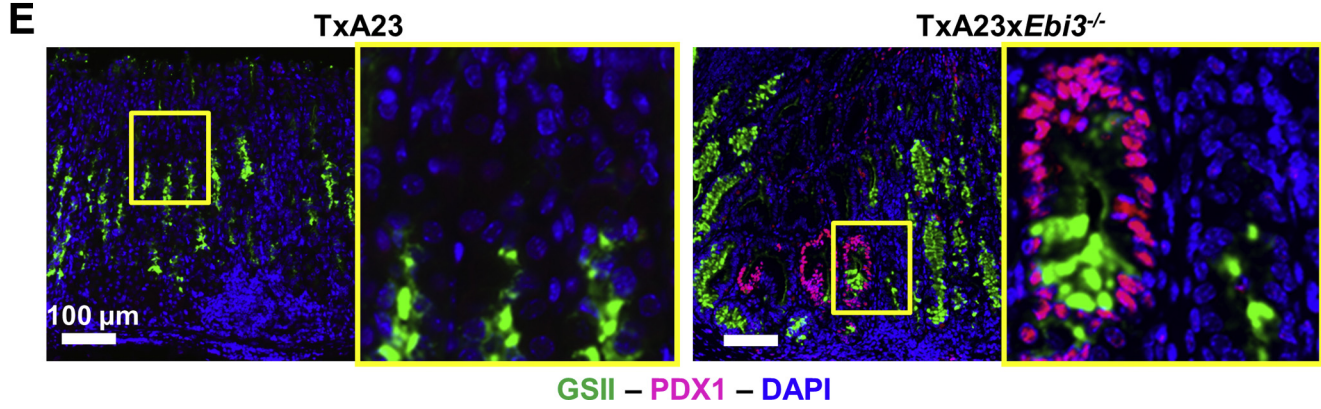
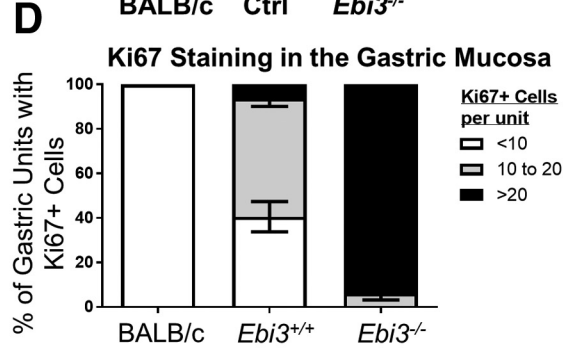
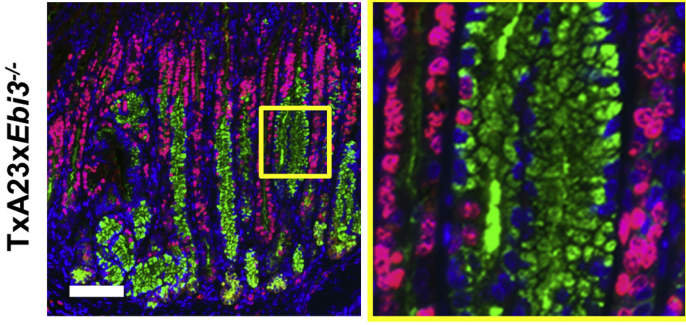
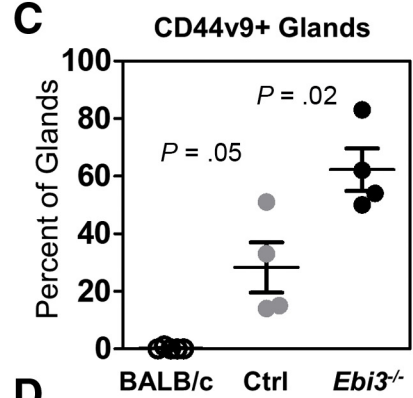
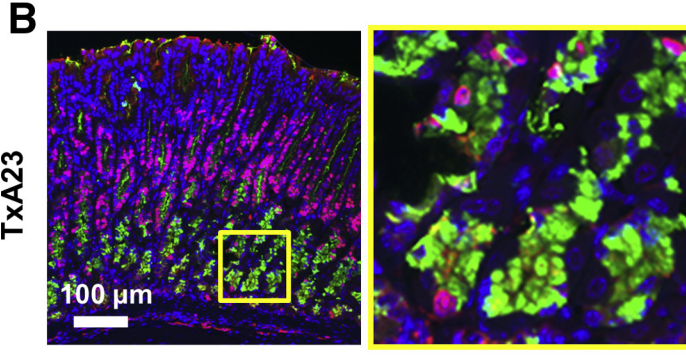
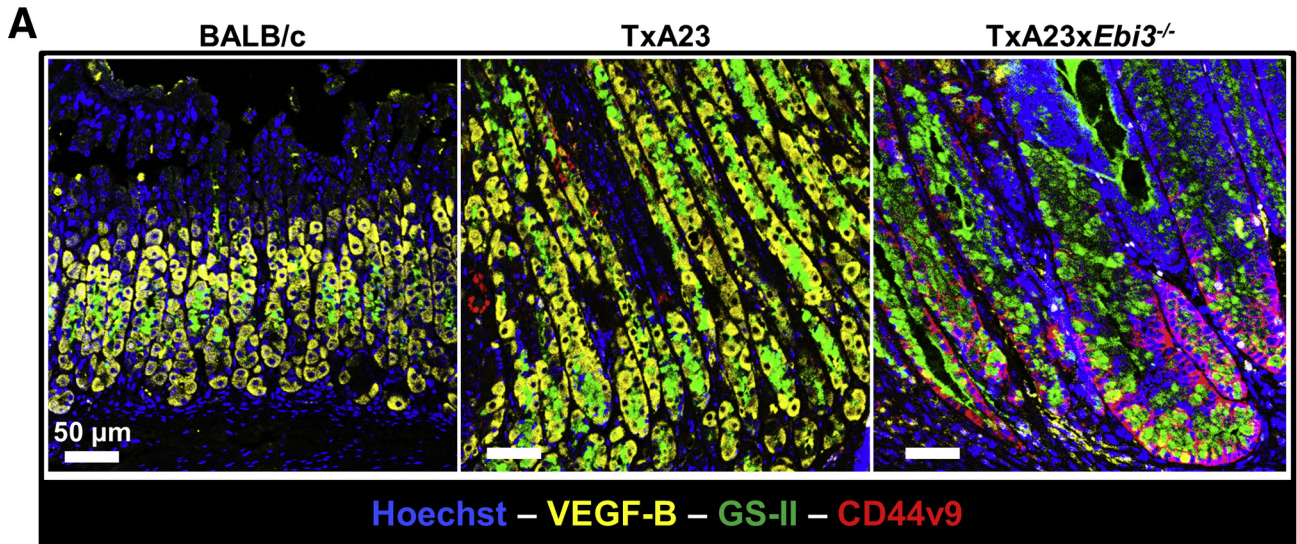
IL27 Is Secreted by Macrophages and Dendritic Cells in the Gastric Mucosa During Atrophic Gastritis

Cytokines made in the gastric mucosa during inflammation likely contribute to the development of preneoplastic changes such as atrophy, hyperplasia, metaplasia, and dysplasia that predispose to carcinogenesis. IL27 plays a protective role in other inflammatory diseases,^{20,33} and recently was detected at high levels in human patients with chronic gastritis.²⁴ We hypothesized that IL27 also may play a protective role during gastritis. To determine whether IL27 was secreted in the gastric mucosa of mice with autoimmune gastritis, we measured IL27 secretion by immune cells in either the draining gastric lymph node or infiltrating the stomach in these mice. Interestingly, we found that IL27 was secreted by mucosa-infiltrating immune cells but was not detectable in the supernatants of lymph node cells (0.2 ± 0.3 vs 59.8 ± 17.5 pg/mL) (Figure 1A), indicating that IL27 could be a critical component of the tissue-specific immune response. To determine which cell types were producing IL27 in the gastric mucosa, we sorted B cells (CD19+), T cells (CD3+), antigen-presenting cells (APCs) (CD19–major histocompatibility complex [MHC] II+), and epithelial cells (epithelial cell adhesion molecule [EpCAM] positive) from the stomachs of mice with chronic gastritis. The expression of *Il27* (encoding p28) and *Ebi3* (encoding EBI3) was measured by quantitative reverse-transcription polymerase chain reaction (qRT-PCR) to determine which immune cell subset expressed the messenger RNA transcripts for both components of the IL27 protein. These analyses showed that APCs had the highest relative expression of both *Il27* and *Ebi3* (Figure 1B). Finally, to determine which cell types were present in the APC population, we used flow cytometry and identified that the IL27-secreting APC population contained CD11b+F4/80+ macrophages and CD11c+ dendritic cells (Figure 1C). These results indicate that IL27 is made by macrophages and dendritic cells in the gastric mucosa during chronic gastritis.

Ebi3 Expression Is Protective During Chronic Atrophic Gastritis

To determine the importance of IL27 in the progression of chronic gastritis, TxA23x*Ebi3*^{-/-} mice that cannot express IL27 were generated and a comparison of gastric pathology between TxA23 and TxA23x*Ebi3*^{-/-} mice was performed. TxA23x*Ebi3*^{-/-} mice developed rapid and more severe gastritis pathology compared with control mice at 2 months of age, at which time TxA23 mice show mild disease pathology (Figure 2A). To compare disease between stomachs from the 2 groups of mice, pathology was scored using a rating system of 0–4, with 0 representing healthy mucosa and 4 representing severe disease pathology, as previously described.^{32,34,35} Stomachs from TxA23x*Ebi3*^{-/-} mice had significantly more severe disease compared with TxA23 mice in all pathologic categories, including inflammation (3.1 ± 0.1 vs 1.4 ± 0.2), parietal cell atrophy (3.5 ± 0.2 vs 1.3 ± 0.2), mucinous hyperplasia/metaplasia (foamy change resembling Brunner's glands in the oxyntic mucosa) (2.8 ± 0.4 vs 0.7 ± 0.2), and mucosal hyperplasia (an increase in the overall thickness of the gastric corpus mucosa) (3.2 ± 0.1 vs 1.6 ± 0.2) (Figure 2B). The TxA23 model has been shown to progress to dysplasia/gastric intraepithelial neoplasia as mice age.³² To determine whether the early development of severe gastritis pathology had implications for the eventual progression to later stages, we analyzed the development of abnormal, dysplasia-like pathology in control and *Ebi3*^{-/-} mice at 1 year of age. Control mice at this time have severe inflammation, atrophy, and hyperplasia/hypertrophy, accompanied by foci of abnormally structured glands that lack the normal mucinous appearance. *Ebi3*^{-/-} mice, however, have a much higher incidence of invasive glandular structures throughout the corpus that infiltrate the submucosa and muscularis. In addition, epithelial cells in *Ebi3*^{-/-} mice lose their normal mucus-filled appearance on H&E, shown nuclear crowding with a loss of basal nuclear localization, and some developed polyp-like appearance not normally seen in the corpus. When scored according to the dysplasia criteria published by Rogers et al.³⁴ TxA23x*Ebi3*^{-/-} had significantly higher scores owing to severe loss of gland orientation, cellular atypia, and visible mitotic figures (0.63 ± 0.5 vs 2.75 ± 0.5) (Figure 2C). The rapid development of severe disease in TxA23x*Ebi3*^{-/-} mice showed that *Ebi3* expression is critical for slowing the progression of inflammation-induced atrophy, hyperplasia, metaplasia, and eventual dysplasia/gastric intraepithelial neoplasia.

Figure 2. (See previous page). Development of inflammation, atrophy, and hyperplasia occurs earlier in *Ebi3*^{-/-} mice. (A) Representative H&E-stained sections of murine gastric corpus from 2-month-old BALB/c, TxA23, and *Ebi3* knockout. Yellow box outlines high-magnification inset showing the degree of inflammation, parietal cell atrophy, mucinous hyperplasia/metaplasia, and mucosal hyperplasia. (B) Pathologic scores for inflammation, parietal cell atrophy, mucinous hyperplasia/metaplasia, and mucosal hyperplasia. Each dot represents the overall score given to 3 areas of gastric corpus from an individual 2-month-old mouse. N = 7–11 mice per group from more than 3 experiments. (C) Representative H&E-stained sections of murine gastric corpus from 12-month-old control TxA23 and TxA23x*Ebi3* knockout mice. Red arrows identify areas in *Ebi3*^{-/-} mice where glandular structures invade the submucosa and muscularis. A red box outlines abnormal branching glands and cellular atypia within the gastric corpus. N = 4 mice per group in at least 2 experiments.



Ebi3 Protects From the Development of Extensive Metaplasia (SPEM) and Increased Epithelial Proliferation

SPEM, in the acute setting, is considered a tissue repair response that resolves after restoration of normal tissue architecture.^{36,37} However, in cases in which the cause of long-lasting mucosal injury is not resolved, such as chronic gastritis, SPEM is associated strongly with, and potentially is the source of, cancer.³⁸ SPEM is identified by co-staining for neck cell markers (Mucin 6 [MUC6]/griffonia simplicifolia [GS]-II lectin), chief cell markers (gastric intrinsic factor [GIF] in mice), and a splice variant of CD44, CD44 variant 9 (CD44v9).^{39–41} Given that *Ebi3*-expressing TxA23 mice are protected from the rapid development of atrophy, it seemed likely that *Ebi3* expression also affected the development of SPEM. To test this, immunofluorescent (IF) staining was performed on the gastric corpus of TxA23 and TxA23x*Ebi3*^{-/-} mice with autoimmune gastritis to evaluate the presence of parietal cells (vascular endothelial growth factor B, yellow), mucous neck cells (GS-II, green), and SPEM cells (CD44v9, red). As expected at this time point, stomachs of TxA23 mice had mild atrophy and patchy development of SPEM in the few completely atrophic glands that were observed (Figure 3A). However, in the stomachs of TxA23x*Ebi3*^{-/-} mice, atrophy was severe and SPEM was observed throughout the gastric corpus. SPEM was assessed quantitatively by IF staining of multiple randomly selected fields of view of the gastric corpus from each mouse (N = 4 mice per group) to determine the percentage of glands that contained CD44v9+ SPEM cells (Figure 3C). These analyses showed that *Ebi3*-expressing mice had significantly less SPEM development compared with *Ebi3*-deficient mice. Because proliferating cells are at increased risk for mutational burden and eventual tumorigenesis, the role of *Ebi3* expression in epithelial proliferation during gastritis also was analyzed. The gastric corpus of wild-type and TxA23x*Ebi3*^{-/-} mice was stained for GS-II (green) and the proliferation marker Ki67 (pink) (Figure 3B). TxA23 mice had a mixed phenotype with normal gland morphology,³² and with intermittent areas of SPEM and hyperplasia in which the number of Ki67+ cells was minimally above normal physiologic levels. However, in the stomachs of TxA23x*Ebi3*^{-/-} mice, there was a significant increase in the proportion of proliferative gastric units in the gastric

mucosa (Figure 3D) (88%–100% of glands having >20 vs 0%–21% of glands having >20). Another metric for the advancement of metaplasia during carcinogenesis was the expression of pancreatic and duodenal homeobox 1 (PDX1), normally an antrum-specific nuclear protein, in the oxyntic mucosal glands.⁴² SPEM regions were assayed in mice for the expression of antralization marker PDX1 (pink) using immunofluorescence (Figure 3E). PDX1+ glands were not detected in control TxA23 mice (left side of Figure 3E); however, PDX1+ glands were observed throughout the gastric corpus of TxA23x*Ebi3*^{-/-} mice. Therefore, these results show that *Ebi3* expression is critical to slow the development of proliferative SPEM during gastritis.

Ebi3 Is Not Required for SPEM in an Acute Chemically Induced Setting

Because *Ebi3* encodes a protein component of IL27,^{18–22,25} and the receptor for this cytokine is expressed on immune cells but not gastric epithelium, we hypothesized that *Ebi3* expression was impacting disease by regulating the type and severity of inflammation. To test this hypothesis, we used an acute, largely noninflammatory, model of atrophy and SPEM development: high-dose tamoxifen (HDT) administration. HDT treatment has been used to rapidly (72 hours) and reversibly induce parietal cell loss to study the mechanisms that underlie preneoplastic epithelial cell changes such as SPEM development in the absence of chronic inflammation.⁴³ BALB/c and BALB/cx*Ebi3*^{-/-} mice were treated with 5 mg HDT per 20 g body weight for 3 days according to published protocols.^{13,43} Importantly, there were no pathologic differences in the gastric epithelium of BALB/c and BALB/cx*Ebi3*^{-/-} mice treated with vehicle. As expected, HDT treatment caused severe atrophy in more than 90% of the gastric corpus in both strains of mice (Figure 4A). IF staining for GIF (yellow) and GS-II (green) was used to assess the extent of SPEM development in HDT-treated mice, showing a significant induction of GIF+GS-II+ cells in both control and *Ebi3*^{-/-} tamoxifen-treated mice compared with vehicle-treated controls (Figure 4B and C). It should be noted that GIF+GS-II+ normal progenitor cells were observed occasionally in the vehicle-treated gastric corpus, but were uncommon enough that the average was less than 1 across 50+ gastric units. SPEM development correlated directly

Figure 3. (See previous page). *Ebi3*^{-/-} mice show more advanced metaplasia (SPEM) with antralization and increased proliferation. (A) Representative immunofluorescent staining of parietal cell atrophy and SPEM development in the gastric corpus of 2-month-old BALB/c, TxA23, and TxA23x*Ebi3*^{-/-} mice. Blue, nuclear stain Hoechst; yellow, parietal cell-specific vascular endothelial growth factor B (VEGF-B); green, neck cell-specific reagent GSII lectin; red, SPEM-specific surface molecule CD44v9. (B) Representative immunofluorescent staining of GSII (green), proliferation marker Ki67 (pink), and nuclear stain 4',6-diamidino-2-phenylindole (DAPI) (blue) in the corpus of TxA23 and TxA23x*Ebi3*^{-/-} mice at 2 months of age. Yellow box indicates high-magnification inset image. (C) Quantitation of the percentage of CD44v9+ glands from multiple fields of view in 4 mice per group from healthy BALB/c mice, control TxA23 mice with chronic gastritis, and TxA23x*Ebi3*^{-/-} mice. (D) Quantitation of Ki67 staining in the gastric corpus of 2-month-old BALB/c, TxA23, and TxA23x*Ebi3*^{-/-} mice as determined by immunofluorescent analysis shown in panel B. N = 6 mice per group from 2 experiments with at least 25 gastric units in 3 separate fields of view analyzed per mouse. Statistical significance was determined using 1-way analysis of variance. (E) Representative immunofluorescent staining of Pdx1+GSII+ SPEM present in the gastric corpus of TxA23 and TxA23x*Ebi3*^{-/-} mice at 2 months of age. Left: GSII (green), Pdx1 (pink), DAPI (blue). Right: GSII (green), Pdx1 (pink), DAPI (blue). Yellow box outlines high-magnification inset image.

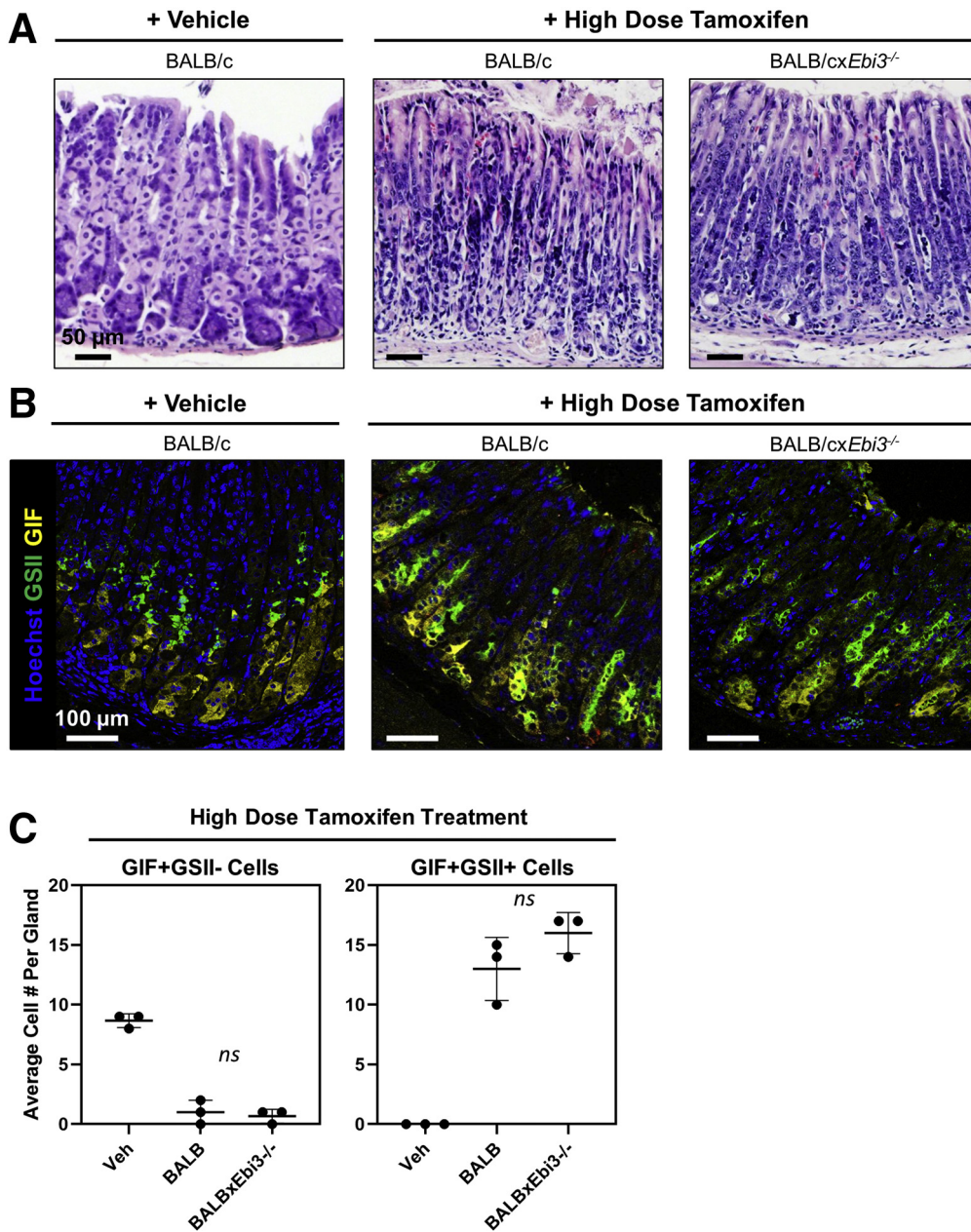


Figure 4. *Ebi3* expression does not influence drug-induced metaplasia development. (A) Representative images of H&E-stained sections of the gastric corpus from vehicle-treated BALB/c, HDT-treated BALB/c, and HDT-treated BALB/cx*Ebi3*^{-/-} mice between 6 and 12 weeks of age showing the degree of parietal cell atrophy induced by tamoxifen relative to vehicle-treated controls. (B) Representative immunofluorescent images of gastric corpus from mice treated as listed earlier. Staining for Hoechst (blue), GIF (yellow), and GSII (green) shows SPEM development. Images are representative of more than 90% of the gastric corpus from 3 mice per experimental group. (C) Quantitation of the average number of GIF+GSII- chief cells (left) and GIF+GSII+ SPEM cells (right) in vehicle-treated BALB/c (Veh) as well as tamoxifen-treated BALB/c and BALB/cx*Ebi3*^{-/-} mice. Calculated from multiple fields of view in 3 mice per group. Data are means \pm SD. Significance was calculated using the Student *t* test.

with atrophy induction in the gastric corpus of both BALB/c and BALB/cx*Ebi3*^{-/-} mice. These experiments determined that *Ebi3* expression does not alter the acute metaplastic response to parietal cell loss, supporting the notion that it regulates chronic inflammation.

*rIL27 Administration Rescues *Ebi3*^{-/-} Mice From Accelerated Development of Atrophy and Metaplasia During Gastritis*

Because IL27 is made in the mucosa during gastritis and *Ebi3*^{-/-} mice have accelerated disease pathology, we hypothesized that IL27 was a protective cytokine during this disease process. However, EBI3 protein is a component of

both IL27 and IL35, so it was crucial to establish that IL27 protected the gastric mucosa from the early development of atrophy and SPEM. To address this, mini osmotic pumps loaded with 4 μ g/mL recombinant, covalently linked p28-EBI3 (rIL27), were implanted subcutaneously into *Ebi3*^{-/-} mice 1 week after weaning. The rIL27 dose was based on previous studies that successfully had prevented other inflammatory diseases using mini osmotic pumps loaded with rIL27.^{20,33} Mice were killed 4 weeks after implantation and the severity of gastritis pathology and metaplasia development was assessed using the pathologic and immunofluorescent methods described previously. The stomachs of rIL27-treated mice were much healthier than those from untreated mice. There was a significant reduction in the

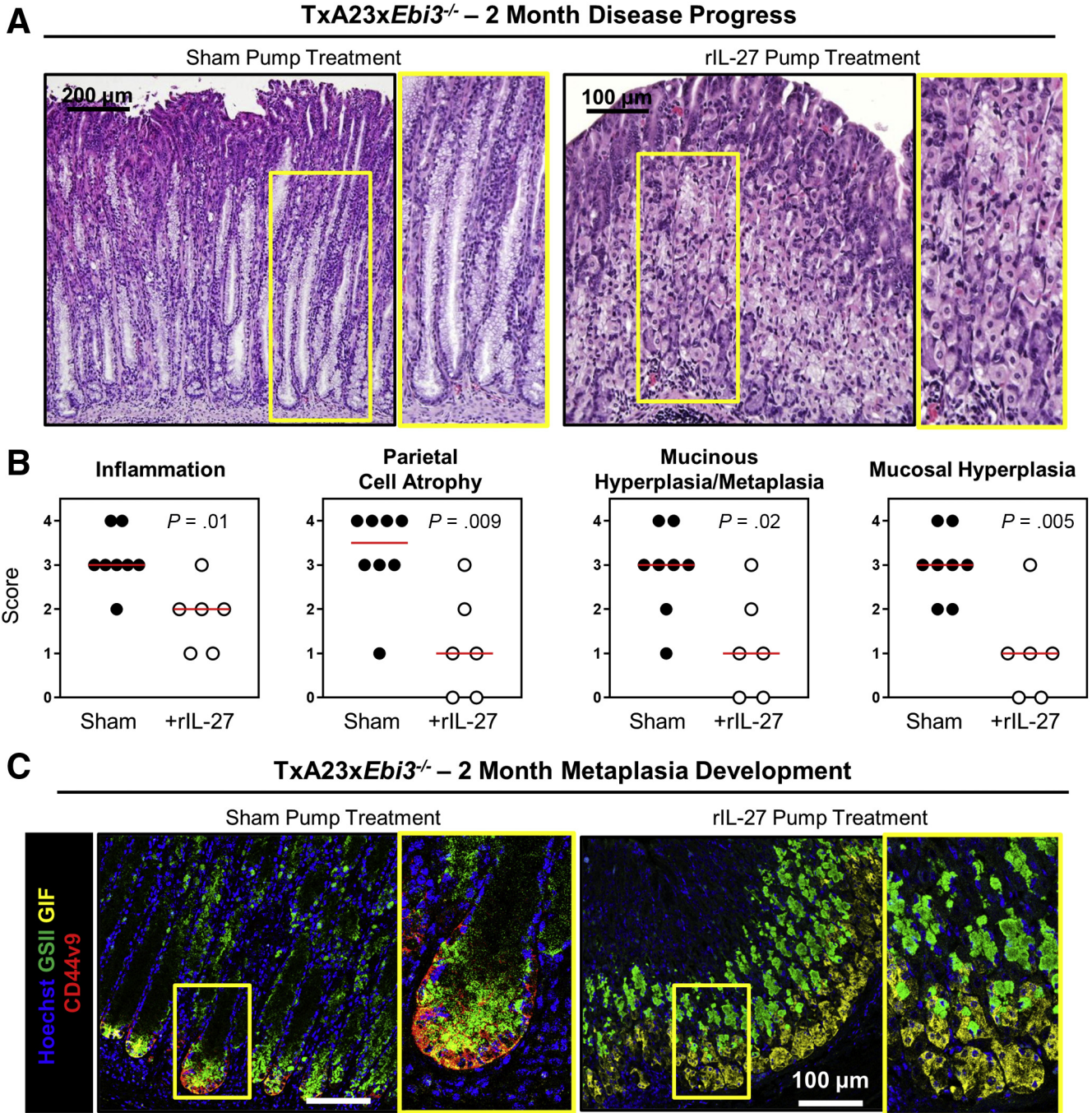


Figure 5. IL27 rescues Ebi3^{-/-} mice from accelerated development of atrophy and metaplasia. (A) Representative images of H&E-stained sections of the gastric corpus from sham pump-treated and rIL27 pump-treated mice at 2 months of age 1 month after pump implantation. *Yellow box* indicates high-magnification *inset* image. (B) Pathologic scores for inflammation, parietal cell atrophy, mucinous hyperplasia/metaplasia, and mucosal hyperplasia. Each *dot* represents the overall score given to 3 areas of gastric corpus from an individual mouse. (C) Representative immunofluorescent staining indicating the extent of SPEM in the gastric corpus of sham control and rIL27-treated mice. Hoechst (blue), GSII (green), GIF (yellow), and CD44v9 (red). *Yellow box* indicates high-magnification *inset* image. N = 6–8 mice per group from 2 separate experiments. Statistical significance was determined using the Mann–Whitney U test.

extent of atrophy, mucinous hyperplasia/metaplasia, and inflammatory infiltrate in H&E-stained sections of gastric corpus from rIL27-treated TxA23xEbi3^{-/-} mice compared with controls (Figure 5A). rIL27-treated mice had significantly lower scores for inflammation (1.8 ± 0.3 vs

3.1 ± 0.2), atrophy (1.2 ± 0.4 vs 3.3 ± 0.4), mucinous hyperplasia/metaplasia (1.2 ± 0.5 vs 2.9 ± 0.4), and mucosal hyperplasia (1.0 ± 0.4 vs 3.0 ± 0.3) (Figure 5B). Immunofluorescent staining was used to assess the degree of SPEM development. There was co-staining of GIF (yellow), GS-II

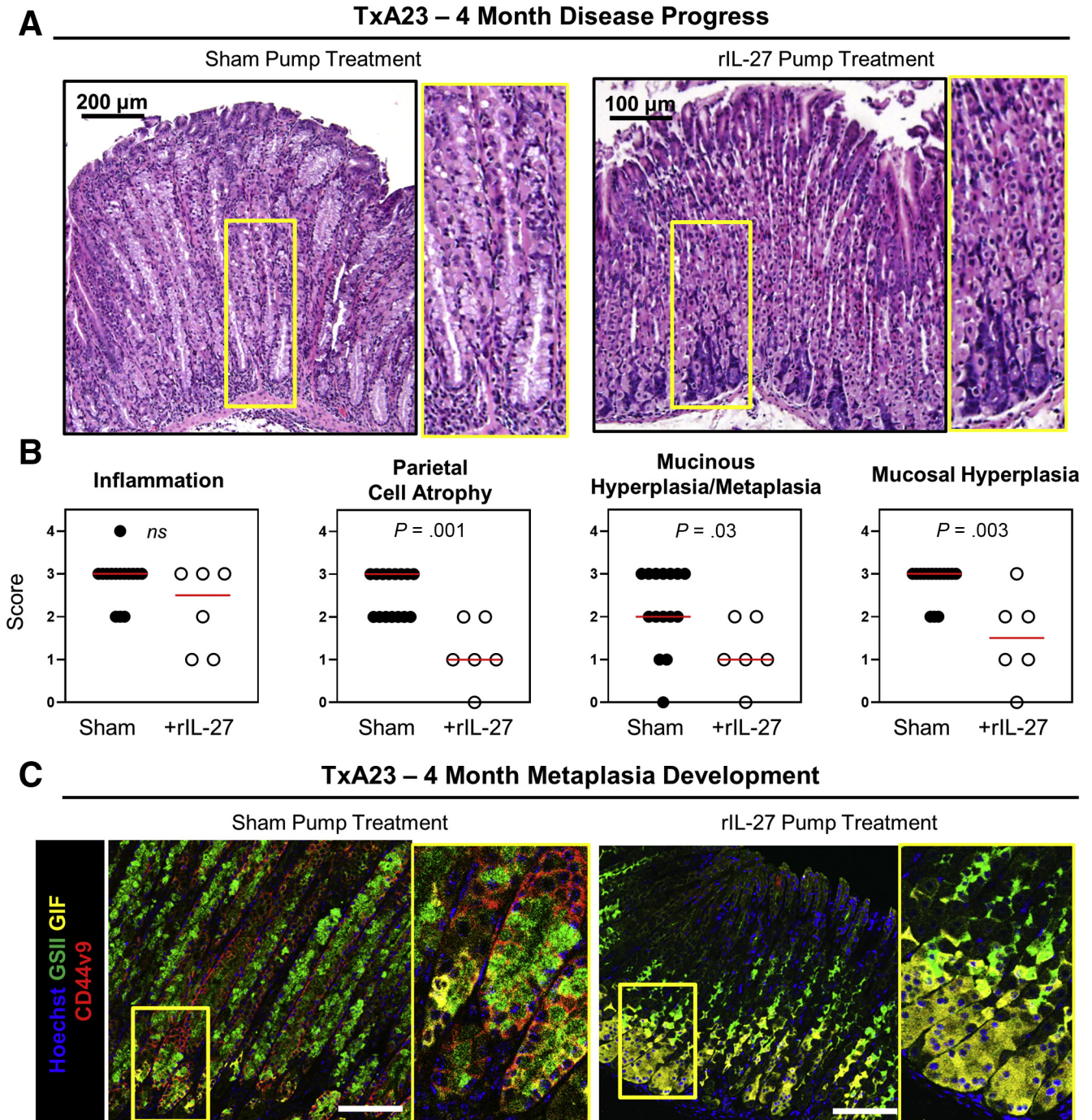


Figure 6. IL27 supplementation reverses atrophy and metaplasia in TxA23 mice with established chronic gastritis. (A) Representative images of H&E-stained sections of the gastric corpus from sham pump-treated and rIL27 pump-treated mice at 4 months of age 1 month after pump implantation. *Yellow box* indicates high-magnification *inset* image. (B) Pathologic scores for inflammation, parietal cell atrophy, mucinous hyperplasia/metaplasia, and mucosal hyperplasia. Each *dot* represents the overall score given to 3 areas of gastric corpus from an individual mouse. (C) Representative immunofluorescent staining indicating the extent of SPEM in the gastric corpus of sham control and rIL27-treated mice. Hoechst (blue), GSII (green), GIF (yellow), and CD44v9 (red). *Yellow box* indicates high-magnification *inset* image. N = 6–8 mice per group from 2 separate experiments. Statistical significance was determined using the Mann–Whitney *U* test.

(green), and CD44v9 (red) diffusely throughout the corpus mucosa of sham-treated mice whereas controls had little to no SPEM development (Figure 5C), corresponding with the pathology scores. These data show that rIL27 is

sufficient to protect *Ebi3*^{-/-} mice from accelerated disease development, showing that the absence of IL27 is the major cause of rapid disease development in TxA23-*Ebi3*^{-/-} mice.

IL27 Supplementation in TxA23 Mice With Ongoing Chronic Gastritis Allows for the Regeneration of Normal Oxyntic Glands

Having shown that rIL27 suppressed atrophy and SPEM development in TxA23x*Ebi3*^{-/-} mice, we next tested whether therapeutic supplementation of rIL27 into TxA23 control mice capable of producing IL27 could suppress disease development. This was tested by implanting mini osmotic pumps to deliver rIL27 into control TxA23 mice at 3 months of age and pathology was evaluated at 4 months of age. Stomachs from rIL27-treated mice were much healthier than controls, in that healthy parietal and chief cells were present in the glands and there was less mucinous hyperplasia/metaplasia throughout the corpus (Figure 6A). Figure 6B shows that although mice treated with rIL27 had similar degrees of inflammation, IL27 treatment significantly decreased the severity of atrophy (2.5 ± 0.5 vs 1.2 ± 0.8), mucinous hyperplasia/metaplasia (2.2 ± 0.9 vs 1.2 ± 0.8), and mucosal hyperplasia (2.8 ± 0.4 vs 1.5 ± 1.0). Finally, immunofluorescent analyses of SPEM in the gastric corpus showed that rIL27-treated mice had a corresponding decrease in SPEM incidence compared with the widespread SPEM present in control mice (Figure 6C). These data showed that increasing IL27 above physiologic levels is an effective way to stop disease progression.

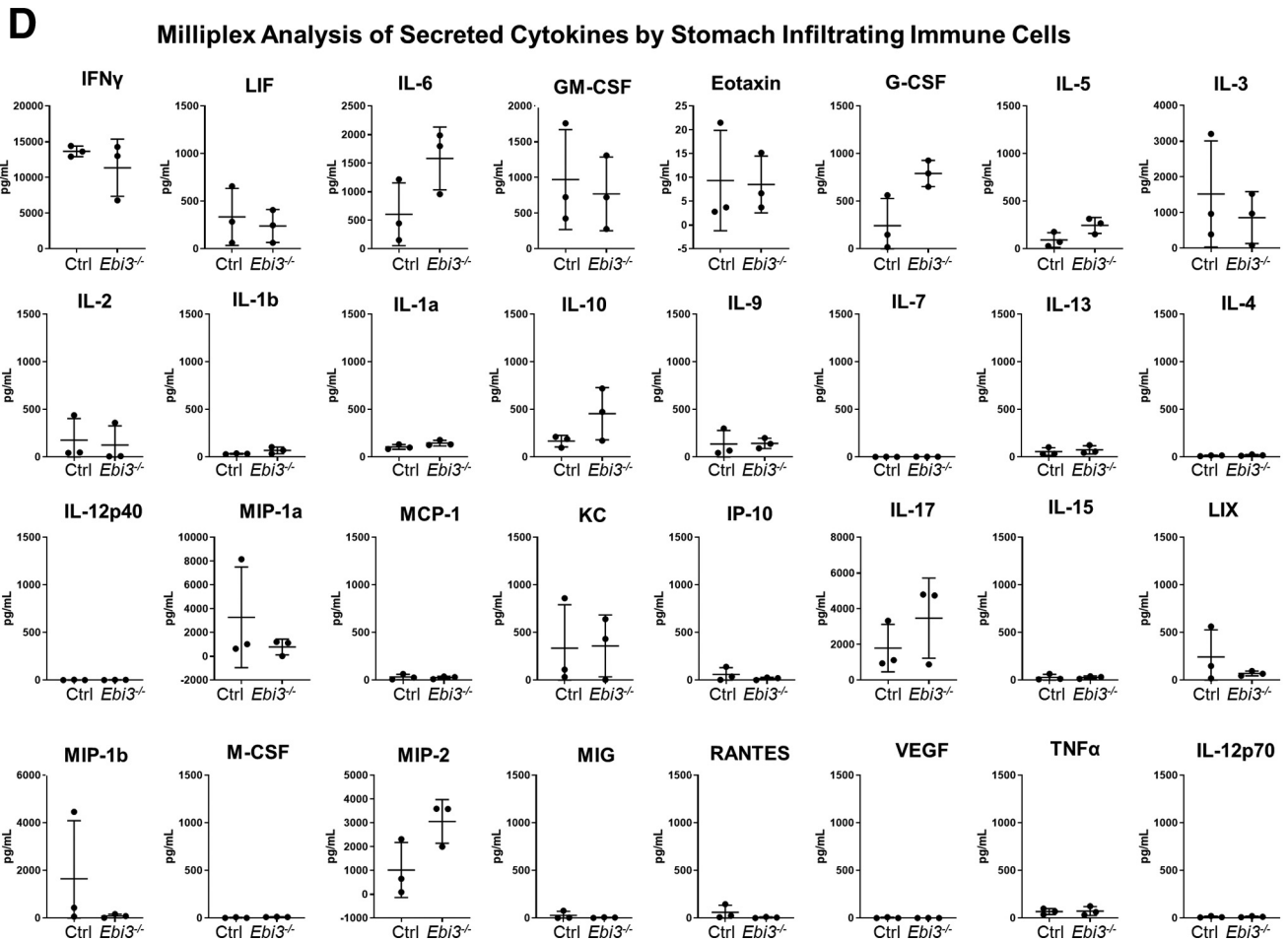
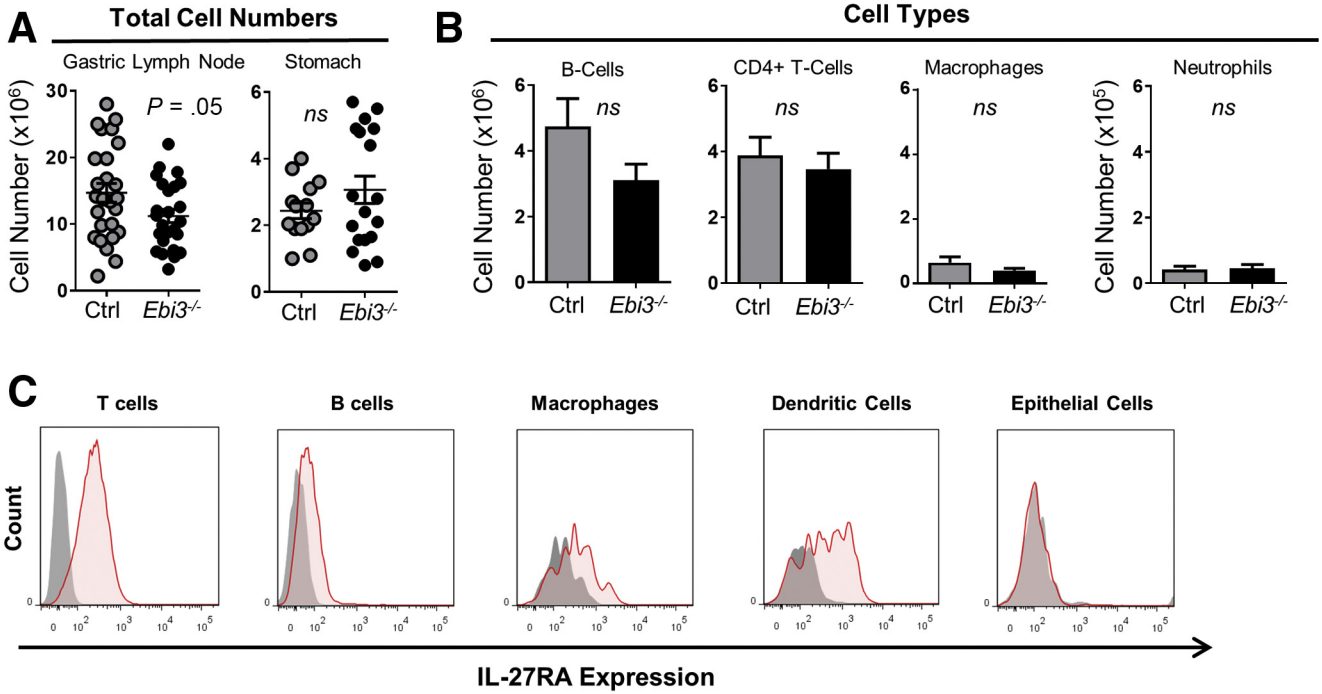
IL27 Acts on Effector CD4⁺ T Cells to Reduce Proinflammatory Gene Expression

IL27 is a pleiotropic cytokine with documented proinflammatory and anti-inflammatory effects on several cell types including but not limited to CD4 T cells, CD8 T cells, regulatory T cells (Tregs), macrophages, and dendritic cells.^{20–22} Therefore, it was critical to determine the cellular target(s) and effect(s) of IL27-mediated suppression of gastritis, but our characterization of the immune response using traditional flow cytometry and bead-based enzyme-linked immunosorbent assay approaches showed that immune cells in control and IL27-deficient mice with gastritis were similar in cell number, proportion of immune cell types (including Th1/Th2/Th17/Treg cells), and cytokine secretion profiles (Figure 7A, B, and D). These data led us to use scRNA sequencing to identify the cell type(s) and transcriptional response(s) to IL27 mediating its protective effect. Three-month-old TxA23 mice were treated with phosphate-buffered saline (PBS) (control) or rIL27-loaded mini osmotic pumps, as in the previous experiments. Immune cells were flushed from the gastric mucosa and subjected to scRNA sequencing and transcriptional profiles of individual cells were analyzed using established bioinformatic pipelines (Seurat 3.0). Although scRNA sequencing does not capture every transcript from every cell, data sets with more than 1000 cells analyzed correlated strongly with traditional bulk RNA sequencing and closely recapitulate bulk transcriptome complexity.^{44,45} These analyses led to the identification of individual immune cell types and the transcription response of each cell type to IL27 treatment. Unsupervised clustering and visualization of approximately 32,000 immune cells identified and separated the immune cells infiltrating the

gastric mucosa, including B cells, CD4 T cells, CD4⁺ Tregs, CD8 T cells, $\gamma\delta$ T cells, natural killer cells, macrophages, mast cells, and *Slfn4*⁺ myeloid—derived suppressor cells, which have been associated with *Helicobacter*-induced gastric metaplasia⁴⁶ (Figure 8A). First, we determined that IL27 receptor (*Il27ra*) transcripts were detected at the highest levels in T-cell clusters. This observation was supported further by traditional flow cytometry staining for IL27RA protein in which T cells had the highest fluorescent intensity, B cells/macrophages/dendritic cells had much lower expression, and epithelial cells did not express any IL27RA protein (Figures 7C and 8B). Next, we compared the gene expression profiles of all cell types between control and IL27-treated mice. Except for CD4⁺ T cells, all other subsets of immune cells were transcriptionally indistinguishable. The CD4 effector cells infiltrating the gastric mucosa of IL27-treated mice had significantly lower expression levels of several genes that are critical for T-cell-mediated inflammation, including chemokines *Ccl5*, *Ccl4*, and *Ccl3*; granule proteins involved in cytotoxicity, *Nkg7* and *Prf1*; receptors for the T-cell growth/activation cytokine IL2 (*Il2rb*); and the inflammation-associated chemokine receptor (*Cxcr6*) (Figure 8C–E).^{47,48} These results identify effector CD4 T cells as the primary targets of IL27, and show that IL27 significantly reduces inflammatory gene expression in these cells.

Discussion

It recently was determined that a novel and potentially autoimmune-mediated gastric corpus adenocarcinoma is increasing in young women in the United States.^{6,7} Autoimmune gastritis traditionally has been associated with neuroendocrine tumors, but the mounting evidence that it also predisposes patients to adenocarcinoma of the corpus is a call for better understanding of how chronic autoimmune inflammation induces precancerous changes and eventual neoplastic transformation. Cytokines serve as critical regulators of immune and epithelial cell functions during chronic inflammation, but the identification and mechanistic understanding of specific cytokines in the regulation of gastritis and gastric precancer still is nascent. A critical observation made in this study and in previous published work is that removal or supplementation of a single cytokine within a complex milieu during autoimmune gastritis resulted in drastic effects on gastritis progression toward carcinogenesis (ie, atrophy and SPEM development). For instance, we previously showed that IL17A neutralization prevents the direct induction of parietal cell apoptosis and decreases gastric atrophy.¹⁶ In addition, IFN γ ,^{17,49,50} IL4,⁵¹ IL13, and IL33⁵² all have been identified as components of the milieu that significantly regulate preneoplastic epithelial cell changes in the stomach. The fact that gastric preneoplasia is sensitive to changes in expression of so many immune factors implies that the types of immune cells and cytokines involved in chronic gastritis likely are playing a critical role in determining the likelihood of carcinogenesis. Therefore, the further identification and mechanistic elucidation of other cellular and soluble components of the gastric inflammatory response will advance the understanding of gastric carcinogenesis significantly.



HDT experiments in this study showed no significant differences in the degree of atrophy or metaplasia development between BALB/c and BALB/cx*Ebi3*^{-/-} mice, indicating that *Ebi3* expression does not affect the epithelial-autonomous mechanisms that cells use to become metaplastic during acute parietal cell ablation,⁵³ but rather is a significant influence during chronic inflammation. The initial observation that TxA23x*Ebi3*^{-/-} mice rapidly develop severe inflammation, parietal cell atrophy, neck cell hyperplasia, as well as diffuse SPEM compared with controls indicates that one of the secreted factors encoded by this gene (IL27 or IL35) is an important suppressive component of the cytokine milieu. Mini osmotic pump restoration of IL27 determined that IL27 protects the gastric mucosa during gastritis. IL27-producing macrophages and dendritic cells infiltrating the gastric tissue were identified. It could be that some macrophages are protective rather than pathogenic during autoimmune gastritis as a result of their expression of IL27, which is an interesting avenue for further research into this critical immune cell compartment. Aside from the macrophage phenotype, this observation lent further credence to the hypothesis that IL27 regulates stomach-specific immunity to control the development of precancerous changes. Interestingly, IL27 production was not found in the draining lymph node, suggesting that IL27 controls on-site immune effector functions rather than immune cell differentiation or priming that occurs in the lymph node. Based on these data, immune cells were flushed from the stomach of untreated and IL27-treated mice, and scRNA sequencing analysis was performed on more than 30,000 cells to determine the stomach-specific targets and effects of IL27 during inflammation.

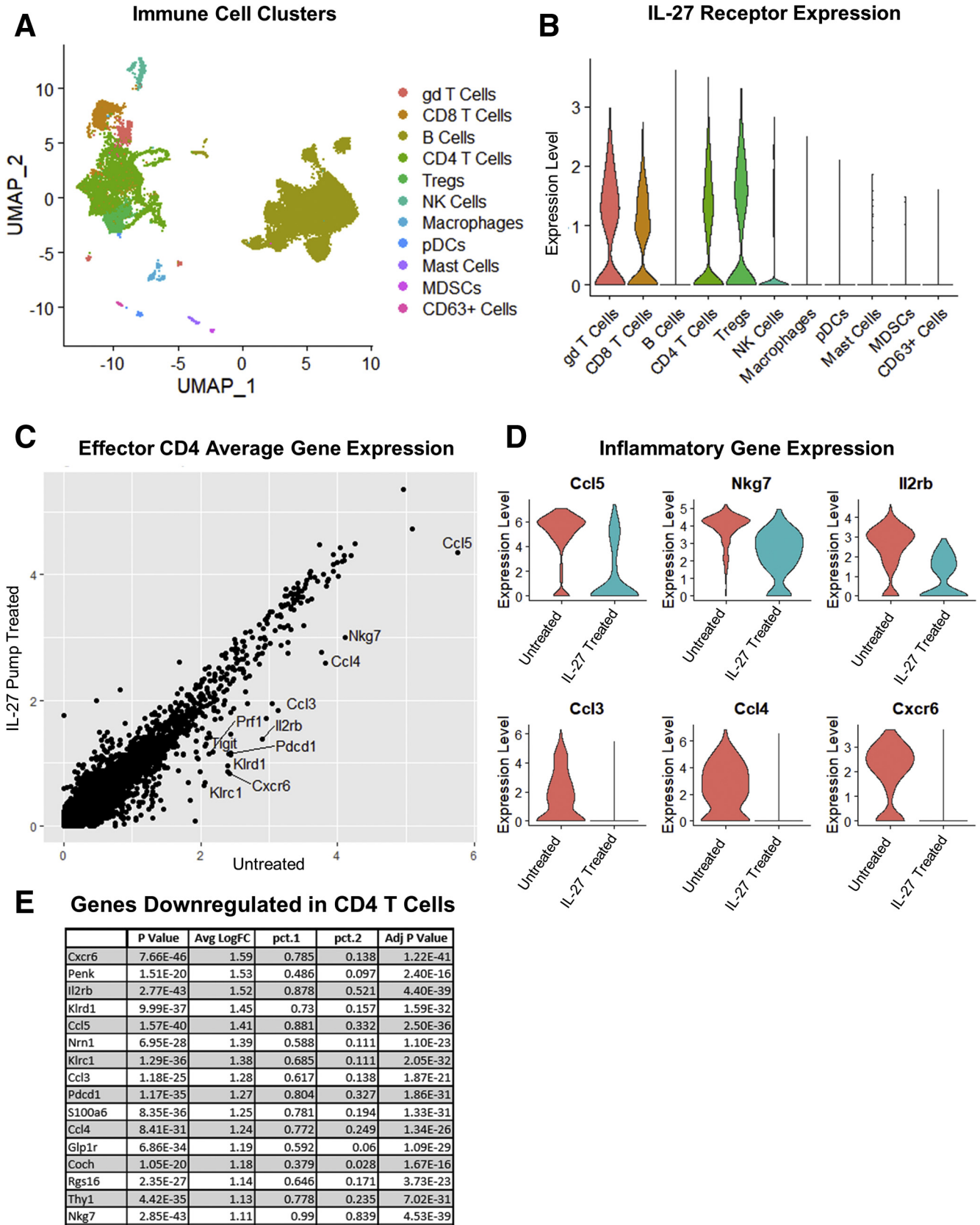
The use of scRNA sequencing allowed for description of the tissue-specific immune response during chronic gastritis including identification of infiltrating immune cell types, determination of cell populations that express the IL27 receptor and thereby are capable of responding to IL27, and also a comparison of the entire captured transcriptome of each cell type between sham-treated and IL27-treated cohorts to determine the unique biological response of each cell type to IL27 during gastritis. Although the receptor for IL27 was found on several T-cell subsets, such as regulatory CD4 T cells and CD8 T cells, these cell types showed no significant alterations in their transcriptomes between the untreated and IL27-treated conditions. Effector CD4 T cells, however, showed the largest and most diverse transcriptional alteration after IL27 supplementation. IL27 suppressed effector CD4

transcripts associated with inflammatory functions including the high-affinity IL2 receptor, cytotoxic granule proteins, and several chemokines that are involved in T-cell activation and effector function. The fact that IL27 specifically suppresses proinflammatory CD4 T cells is critical because CD4 T cells are the mediators of gastritis in both autoimmunity and *Helicobacter* infection in mouse models and in human patients.

The fact that systemic administration of IL27 suppressed tissue damage to the extent that normal oxyntic glands were restored suggests that immunotherapeutic manipulation of the cytokine milieu and infiltrating CD4 T cells during gastritis could yield significant clinical benefits. Although recombinant cytokines are difficult to use therapeutically for a number of reasons, identification of which effector CD4 gene(s) suppressed by IL27 signaling are critical drivers of disease progression is a promising avenue for future study, perhaps by performing bulk RNA sequencing of sorted CD4 T cells from mice treated with IL27, because these effector functions may serve as useful biomarkers of individuals at risk for carcinogenesis. In addition, progress in this area could provide cytokine mimetics or neutralizing antibodies capable of treating metaplasia after it has developed. However, an important limitation of this study was that it uses a mouse model of autoimmune gastritis. Although autoimmune gastritis is associated with an increased risk of gastric adenocarcinoma similar to *H. pylori* infection,⁵ further studies of this cytokine in other model systems are needed to broaden the conclusions of this article beyond the autoimmune setting.

These data show that IL27 suppresses the development of gastric precancer (atrophy and SPEM) in a setting of chronic autoimmune inflammation, and even allows for tissue regeneration if administered after the lesions have developed. However, it is unclear what role IL27 plays after tumorigenesis takes place. After development of a solid tumor, production of IL27 may inhibit antitumor immunity.⁵⁴ Indeed, although IL27 was detected at high levels in gastric tissue from human patients with *H. pylori*-induced gastritis, IL27 was not detected in the tissue of gastric cancer patients.²⁴ This temporal change in IL27 expression based on disease stage (eg, gastritis vs gastric adenocarcinoma) suggests that these same immunoregulatory activities that prevent carcinogenesis during inflammation are harmful after tumorigenesis. In addition, the role of IL35 in this disease process requires further exploration. These studies undoubtedly show that IL27 is protective during autoimmune gastritis and, based on the complete rescue of the

Figure 7. (See previous page). **Control and *Ebi3*^{-/-} mice with autoimmune gastritis have similar immune cell numbers, proportions, and cytokine secretion profiles.** (A) Total immune cell numbers isolated from the gastric lymph node (left) and the gastric mucosa (right). Each dot represents 1 mouse, with 15–20 mice per group. (B) Total numbers of immune cell subsets in control and *Ebi3*^{-/-} TxA23 mice, with 15–20 mice per group. (C) Representative flow cytometry histograms of IL27RA staining on different immune subsets (red) compared with IL27RA-deficient controls (gray), with 4–6 mice per group. (D) Analysis of cytokines secreted by stomach-infiltrating immune cells that have been restimulated in vitro with PMA/ionomycin for 72 hours. Supernatants were analyzed using a Milliplex bead-based cytokine assay (EMDMillipore; Burlington, MA). There were 3 mice per group. Significance was calculated using the Student *t* test. Ctrl, control; G-CSF, Granulocyte colony stimulating factor; IP-10, Interferon-induced protein 10; KC, Keratinocyte chemoattractant; LIF, Leukocyte inhibitory factor; LIX, LPS induced CXC chemokine; M-CSF, macrophage colony stimulating factor; MCP-1, monocyte chemoattractant protein 1; MIG, monokine induced by gamma interferon; MIP, macrophage inflammatory protein; PMA, Phorbol 12-myristate 13-acetate; RANTES, Regulated upon Activation, Normal T Cell Expressed and Presumably Secreted; VEGF, vascular endothelial growth factor.



accelerated phenotype we observed in *Ebi3*^{-/-} mice by rIL27, we hypothesize that the role of IL35 is likely to be minimal. However, interpretation of these results still is somewhat limited by the lack of a direct treatment of mice with rIL35, and further studies of IL35 in this context are warranted to determine if this poorly understood cytokine plays a role. A greater understanding of how to manipulate the immune system, both before and after solid tumor formation, could provide critical clinical advances in the identification of at-risk individuals, early diagnosis of cancers, and novel immunotherapeutic techniques.

Materials and Methods

Mice

TxA23 mice express a transgenic T-cell receptor specific for a peptide from H⁺/K⁺ adenosine triphosphatase α chain on a BALB/c background, and have been described previously.^{31,32,55,56} TxA23 mice were bred onto a BALB/*cxEbi3*^{-/-} background using mice purchased from Jackson Laboratories (Bar Harbor, ME). All mice were maintained in our animal facility and cared for in accordance with institutional guidelines. Studies were performed on a mixed group of male and female mice with co-housed littermate controls. For pump implantation studies, 800 ng of carrier-free rIL27 (2799-ML-010/CF; R&D Systems, Minneapolis, MN) in 200 μ L of sterile PBS was loaded into mini osmotic pumps (model 2004; Alzet, Cupertino, CA) based on published effective doses in mice.^{20,33} Pumps were implanted subcutaneously into TxA23*Ebi3*^{-/-} upon reaching a 20 g minimum weight (at approximately 5 weeks of age) or into control TxA23 mice at 3 months of age. Mice were killed 4 weeks after implantation. Pumps containing only sterile PBS were used as sham controls.

Histopathology

Stomachs were removed from mice, rinsed in saline, immersion-fixed in 10% neutral-buffered formalin, paraffin embedded, sectioned, and stained with H&E. For scoring, investigators were blinded, and sections from individual mice were assigned scores between 0 (absent) and 4 (severe) to indicate the severity of inflammation, oxyntic atrophy, mucinous hyperplasia/metaplasia, and mucosal hyperplasia.^{32,34}

Immunofluorescence

Stomachs were prepared, stained, and imaged using methods modified from Ramsey et al.⁵⁷ The primary antibodies used for immunostaining were goat anti-vascular endothelial growth factor B (1:100, sc-13083; Santa Cruz

Biotechnology, Dallas, TX), anti-CD44v9 (1:10,000, LKGM002; Cosmo Bio, Carlsbad, CA), and goat anti-GIF (1:10,000; a gift from David Alpers, Washington University in St. Louis). After washing, sections were incubated with secondary antibodies and GS-II lectin (1:500, L21415; ThermoFisher, Waltham, MA). Sections were washed, stained with Hoechst (62249; ThermoFisher) 1:20,000 in PBS, and mounted in ProLong Gold Antifade mountant (P36934; ThermoFisher).

Flow Cytometry

Cell surface staining was performed according to standard procedures using antibodies against CD4 (562891; BD Pharmingen, San Jose, CA), CD8 (563046; BD Horizon, San Jose, CA), CD19 (551001; BD Pharmingen), CD11b (550993; BD Pharmingen), CD11c (550261; BD Pharmingen), F4/80 (123147; BioLegend), and MHC II. All flow cytometry was performed on a BD LSRII (BD Biosciences, San Jose, CA) and analyzed using FlowJo (BD Biosciences, Ashland, OR).

HDT Treatment

The use of HDT to induce parietal cell atrophy and SPERM development has been described previously.^{13,36,43} Tamoxifen (5 mg/20 g body weight, T006000; Toronto Research Chemicals, North York, ON) was injected intraperitoneally once daily for 3 days. Tamoxifen was dissolved in a vehicle of 10% ethanol and 90% sunflower oil (S5007; Millipore Sigma, St. Louis, MO). Determination of metaplasia induction was performed by looking at 3 sections of gastric corpus per mouse, in at least 3 mice per group.

Cell Sorting and qRT-PCR

After isolation from the gastric mucosa, cells were stained with anti-CD45 BV786, anti-CD90 BV711 (563772; BD Horizon), anti-MHC II AF488 (562352; BD Pharmingen), anti-CD19 APC (550992; BD Pharmingen), and anti-EpCAM APC ef780 (47-5791-81; Invitrogen), and sorted using a BD FACSAria (BD Biosciences, San Jose, CA) into the following groups: CD45-EpCAM+, CD45+CD19+MHC II+, CD45+CD19-MHC II+, and CD45+MHC II-CD90+. After sorting, cells were restimulated overnight with phorbol myristate acetate (25 ng/mL) and ionomycin (0.5 ng/mL). RNA was isolated the following morning using a RNeasy Mini Kit (74104; Qiagen, Germantown, MD). Complementary DNA (cDNA) was generated using a high-capacity reverse-transcription kit (4368814; ThermoFisher). The *Gapdh*, *Il27*, and *Ebi3* message was measured using TaqMan primer probes according to the manufacturer's specifications (*Gapdh*: Mm99999915_g1; *Il27*: Mm00461164_m1; and

Figure 8. (See previous page). IL27 acts on effector CD4 T cells to reduce inflammatory gene expression during autoimmune gastritis. Immune cells were flushed and sort-purified from the gastric mucosa of sham-treated and IL27-treated mice and subjected to scRNA sequencing analysis. (A) Uniform Manifold Approximation and Projection clustering of approximately 32,000 immune cells sequenced. Each dot is an individual cell. Cells are colored by cluster identity. (B) *Il27ra* expression in sequenced immune cell clusters. (C) Dot plot of the relative expression of all detected transcripts calculated from the per-cell average relative expression from effector CD4 T cells identified in the untreated and IL27-treated libraries. (D) Corresponding violin plots showing expression level of selected inflammatory genes in that effector CD4 T-cell subset. (E) Select genes significantly down-regulated by IL27 treatment in CD4⁺ T cells. MDSC, Myeloid derived suppressor cells; NK, natural killer; pDC, peripheral dendritic cells.

Ebi3: Mm00469294_m1; ThermoFisher). Expression was reported as target relative to *Gapdh* for each sample. For scRNA sequencing analysis, CD45+ propidium iodide cells were sorted from the gastric mucosa to separate live immune cells from dead and epithelial cells. These cell suspensions then were washed once and loaded onto the 10× Genomics Chromium Controller according to the manufacturer's recommendations.

Chromium Single-Cell 5' Library Construction

The Chromium Single-Cell Controller instrument (10× Genomics, Pleasanton, CA) was used in these studies according to recommended manufacturer protocols and has been described previously.⁵⁸ Briefly, gastric corpus epithelial single-cell suspensions were loaded on a Chromium Single-Cell Controller instrument to generate single-cell gel beads in emulsion. scRNA sequencing libraries were prepared using the Chromium Single-Cell 5' Library and Gel Bead Kit (P/N 1000006; 10× Genomics). RT of gel beads in emulsion was performed in a Veriti 96-Well Thermal cycler (4375786; Applied Biosystems, Foster City, CA): 53°C for 45 minutes, 85°C for 5 minutes, held at 4°C, and stored at -20°C. The gel beads in emulsion then were broken, and the single-strand cDNA was cleaned up with DynaBeads MyOne Silane Beads (P/N 37002D; ThermoFisher, Waltham, MA). Barcoded, full-length cDNA was amplified using the Veriti 96-Well Thermal Cycler: 98°C for 45 seconds, cycled 13×: 98°C for 20 seconds, 67°C for 30 seconds, and 72°C for 1 minute, then 72°C for 1 minute, held at 4°C. The amplified cDNA product was cleaned up with the SPRIselect Reagent Kit (0.6 × SPRI, P/N B23318; Beckman Coulter). 5' gene expression libraries were constructed using the reagents in the Chromium Single-Cell 3'/5' Library Construction kit (P/N 1000020). For 5' gene expression library construction, these steps were followed: (1) fragmentation, end repair and A-tailing; (2) after fragmentation, end repair and A-tailing cleanup with SPRIselect; (3) adaptor ligation; (4) after ligation clean-up with SPRIselect; and (5) sample index PCR and clean-up. Final quality control and Illumina sequencing of the prepared libraries was performed by the Washington University in St. Louis Genome Technology Access Center.

scRNA Sequencing Data Processing and Statistical Analysis

Raw data were processed through the CellRanger 3.0 pipeline (10× Genomics) and secondary clustering and differential expression analysis were conducted in Seurat/R.⁵⁹ Before clustering, all libraries and subsets were processed to ensure quality. Genes relating to mitochondrial proteins are markers for broken or low-quality cells.⁶⁰ Consequently, low-quality cells expressing high levels of mitochondrial markers above a majority threshold unique to each library/subset were filtered out before downstream analysis. Each library then globally was scaled and normalized by a scale factor of 1×10^4 and log transformation. In addition, unwanted sources of variation attributed to biological noise and batch effect were

identified and regressed out to improve downstream analysis and dimensionality reduction.⁶¹

Components for clustering were generated by canonical correlation analysis. High-signal canonical correlates explaining the most variance in comparison identity classes were aligned by dynamic time warping, and their dimensions were used for subsequent shared nearest neighbor clustering and visualization by uniform manifold approximation and projection for dimension reduction.^{62,63} Globally distinguishing genes for each cluster and comparison identity class were identified by calculating the normalized gene expression for the average single cell. Significant genes with at least a 2-fold change and a corrected *P* value less than .01 were identified via the Wilcoxon rank-sum test with Bonferroni correction for multiple comparisons.

Other Statistical Analysis

Data are expressed as means of individual determinations ± standard error. Statistical analysis was performed by either the Mann–Whitney *U* test or an unpaired Student *t*-test using GraphPad Prism 8 (GraphPad, San Diego, CA).

References

1. Fox JG, Wang TC. Inflammation, atrophy, and gastric cancer. *J Clin Invest* 2007;117:60–69.
2. Ferlay J, Soerjomataram I, Dikshit R, Eser S, Mathers C, Rebelo M, Parkin DM, Forman D, Bray F. Cancer incidence and mortality worldwide: sources, methods and major patterns in GLOBOCAN 2012. *Int J Cancer* 2015;136:E359–E386.
3. Hooi JKY, Lai WY, Ng WK, Suen MMY, Underwood FE, Tanyingoh D, Malfertheiner P, Graham DY, Wong VW, Wu JCY, Chan FKL, Sung JJY, Kaplan GG, Ng SC. Global prevalence of *Helicobacter pylori* Infection: systematic review and meta-analysis. *Gastroenterology* 2017;153:420–429.
4. Landgren AM, Landgren O, Gridley G, Dores GM, Linet MS, Morton LM. Autoimmune disease and subsequent risk of developing alimentary tract cancers among 4.5 million US male veterans. *Cancer* 2011;117:1163–1171.
5. Mahmud N, Stashek K, Katona BW, Tondon R, Shroff SG, Roses R, Furth EE, Metz DC. The incidence of neoplasia in patients with autoimmune metaplastic atrophic gastritis: a renewed call for surveillance. *Ann Gastroenterol* 2019;32:67–72.
6. Anderson WF, Rabkin CS, Turner N, Fraumeni JF Jr, Rosenberg PS, Camargo MC. The changing face of noncardia gastric cancer incidence among US non-Hispanic whites. *J Natl Cancer Inst* 2018;110:608–615.
7. Blaser MJ, Chen Y. A new gastric cancer among us. *J Natl Cancer Inst* 2018;110:549–550.
8. Stummvoll GH, DiPaolo RJ, Huter EN, Davidson TS, Glass D, Ward JM, Shevach EM. Th1, Th2, and Th17 effector T cell-induced autoimmune gastritis differs in pathological pattern and in susceptibility to suppression by regulatory T cells. *J Immunol* 2008;181:1908–1916.
9. Correa P. A human model of gastric carcinogenesis. *Cancer Res* 1988;48:3554–3560.

10. Correa P, Piazzuelo MB. The gastric precancerous cascade. *J Dig Dis* 2012;13:2–9.
11. Yamaguchi H, Goldenring JR, Kaminishi M, Lee JR. Identification of spasmolytic polypeptide expressing metaplasia (SPEM) in remnant gastric cancer and surveillance postgastrectomy biopsies. *Dig Dis Sci* 2002; 47:573–578.
12. Lennerz JK, Kim SH, Oates EL, Huh WJ, Doherty JM, Tian X, Bredemeyer AJ, Goldenring JR, Lauwers GY, Shin YK, Mills JC. The transcription factor *MIST1* is a novel human gastric chief cell marker whose expression is lost in metaplasia, dysplasia, and carcinoma. *Am J Pathol* 2010;177:1514–1533.
13. Burclaff J, Osaki LH, Liu D, Goldenring JR, Mills JC. Targeted apoptosis of parietal cells is insufficient to induce metaplasia in stomach. *Gastroenterology* 2017; 152:762–766 e7.
14. Petersen CP, Weis VG, Nam KT, Sousa JF, Fingleton B, Goldenring JR. Macrophages promote progression of spasmolytic polypeptide-expressing metaplasia after acute loss of parietal cells. *Gastroenterology* 2014; 146:1727–1738 e8.
15. Weis VG, Sousa JF, LaFleur BJ, Nam KT, Weis JA, Finke PE, Ameen NA, Fox JG, Goldenring JR. Heterogeneity in mouse spasmolytic polypeptide-expressing metaplasia lineages identifies markers of metaplastic progression. *Gut* 2013;62:1270–1279.
16. Bockerstett KA, Osaki LH, Petersen CP, Cai CW, Wong CF, Nguyen TM, Ford EL, Hoft DF, Mills JC, Goldenring JR, DiPaolo RJ. Interleukin-17A promotes parietal cell atrophy by inducing apoptosis. *Cell Mol Gastroenterol Hepatol* 2018;5:678–690 e1.
17. Osaki LH, Bockerstett KA, Wong CF, Ford EL, Madison BB, DiPaolo RJ, Mills JC. Interferon-gamma directly induces gastric epithelial cell death and is required for progression to metaplasia. *J Pathol* 2019; 247:513–523.
18. Muallem G, Wagage S, Sun Y, DeLong JH, Valenzuela A, Christian DA, Harms Pritchard G, Fang Q, Buza EL, Jain D, Elloso MM, Lopez CB, Hunter CA. IL-27 limits type 2 immunopathology following parainfluenza virus infection. *PLoS Pathog* 2017;13:e1006173.
19. Lucas S, Ghilardi N, Li J, de Sauvage FJ. IL-27 regulates IL-12 responsiveness of naive CD4⁺ T cells through Stat1-dependent and -independent mechanisms. *Proc Natl Acad Sci U S A* 2003;100:15047–15052.
20. Do JS, Visperas A, Sanogo YO, Bechtel JJ, Dvorina N, Kim S, Jang E, Stohlman SA, Shen B, Fairchild RL, Baldwin WM III, Vignali DA, Min B. An IL-27/Lag3 axis enhances Foxp3⁺ regulatory T cell-suppressive function and therapeutic efficacy. *Mucosal Immunol* 2016; 9:137–145.
21. Mascanfroni ID, Yeste A, Vieira SM, Burns EJ, Patel B, Sloma I, Wu Y, Mayo L, Ben-Hamo R, Efroni S, Kuchroo VK, Robson SC, Quintana FJ. IL-27 acts on DCs to suppress the T cell response and autoimmunity by inducing expression of the immunoregulatory molecule CD39. *Nat Immunol* 2013;14:1054–1063.
22. Wehrens EJ, Wong KA, Gupta A, Khan A, Benedict CA, Zuniga EI. IL-27 regulates the number, function and cytotoxic program of antiviral CD4 T cells and promotes cytomegalovirus persistence. *PLoS One* 2018;13: e0201249.
23. Visperas A, Do JS, Bulek K, Li X, Min B. IL-27, targeting antigen-presenting cells, promotes Th17 differentiation and colitis in mice. *Mucosal Immunol* 2014;7:625–633.
24. Rocha GA, de Melo FF, Cabral M, de Brito BB, da Silva FAF, Queiroz DMM. Interleukin-27 is abrogated in gastric cancer, but highly expressed in other *Helicobacter pylori*-associated gastroduodenal diseases. *Helicobacter* 2020;25:e12667.
25. Fitzgerald DC, Ciric B, Touil T, Harle H, Grammatikopoulou J, Das Sarma J, Gran B, Zhang GX, Rostami A. Suppressive effect of IL-27 on encephalitic Th17 cells and the effector phase of experimental autoimmune encephalomyelitis. *J Immunol* 2007; 179:3268–3275.
26. Meka RR, Venkatesha SH, Dudics S, Acharya B, Moudgil KD. IL-27-induced modulation of autoimmunity and its therapeutic potential. *Autoimmun Rev* 2015; 14:1131–1141.
27. Collison LW, Workman CJ, Kuo TT, Boyd K, Wang Y, Vignali KM, Cross R, Sehy D, Blumberg RS, Vignali DA. The inhibitory cytokine IL-35 contributes to regulatory T-cell function. *Nature* 2007;450:566–569.
28. Do J, Kim D, Kim S, Valentin-Torres A, Dvorina N, Jang E, Nagarajavel V, DeSilva TM, Li X, Ting AH, Vignali DAA, Stohlman SA, Baldwin WM 3rd, Min B. Treg-specific IL-27 α deletion uncovers a key role for IL-27 in Treg function to control autoimmunity. *Proc Natl Acad Sci U S A* 2017;114:10190–10195.
29. Casella G, Finardi A, Descamps H, Colombo F, Maiorino C, Ruffini F, Patrone M, Degano M, Martino G, Muzio L, Becher B, Furlan R. IL-27, but not IL-35, inhibits neuroinflammation through modulating GM-CSF expression. *Sci Rep* 2017;7:16547.
30. Nguyen QT, Jang E, Le HT, Kim S, Kim D, Dvorina N, Aronica MA, Baldwin WM 3rd, Asosingh K, Comhair S, Min B. IL-27 targets Foxp3⁺ Tregs to mediate anti-inflammatory functions during experimental allergic airway inflammation. *JCI Insight* 2019;4.
31. McHugh RS, Shevach EM, Margulies DH, Natarajan K. A T cell receptor transgenic model of severe, spontaneous organ-specific autoimmunity. *Eur J Immunol* 2001;31:2094–2103.
32. Nguyen TL, Khurana SS, Bellone CJ, Capoccia BJ, Sagartz JE, Kesman RA Jr, Mills JC, DiPaolo RJ. Auto-immune gastritis mediated by CD4⁺ T cells promotes the development of gastric cancer. *Cancer Res* 2013; 73:2117–2126.
33. Kim D, Le HT, Nguyen QT, Kim S, Lee J, Min B. Cutting edge: IL-27 attenuates autoimmune neuroinflammation via regulatory T cell/Lag3-dependent but IL-10-independent mechanisms in vivo. *J Immunol* 2019; 202:1680–1685.
34. Rogers AB, Taylor NS, Whary MT, Stefanich ED, Wang TC, Fox JG. *Helicobacter pylori* but not high salt induces gastric intraepithelial neoplasia in B6129 mice. *Cancer Res* 2005;65:10709–10715.

35. Bockerstett KA, Wong CF, Koehm S, Ford EL, DiPaolo RJ. Molecular characterization of gastric epithelial cells using flow cytometry. *Int J Mol Sci* 2018; 19.
36. Huh WJ, Khurana SS, Geahlen JH, Kohli K, Waller RA, Mills JC. Tamoxifen induces rapid, reversible atrophy, and metaplasia in mouse stomach. *Gastroenterology* 2012;142:21–24 e7.
37. Engevik AC, Feng R, Choi E, White S, Bertaux-Skeirik N, Li J, Mahe MM, Aihara E, Yang L, DiPasquale B, Oh S, Engevik KA, Giraud AS, Montrose MH, Medvedovic M, Helmrath MA, Goldenring JR, Zavros Y. The development of spasmolytic polypeptide/TFF2-expressing metaplasia (SPEM) during gastric repair is absent in the aged stomach. *Cell Mol Gastroenterol Hepatol* 2016; 2:605–624.
38. Mills JC, Sansom OJ. Reserve stem cells: differentiated cells reprogram to fuel repair, metaplasia, and neoplasia in the adult gastrointestinal tract. *Sci Signal* 2015;8:re8.
39. Bertaux-Skeirik N, Wunderlich M, Teal E, Chakrabarti J, Biesiada J, Mahe M, Sundaram N, Gabre J, Hawkins J, Jian G, Engevik AC, Yang L, Wang J, Goldenring JR, Qualls JE, Medvedovic M, Helmrath MA, Diwan T, Mulloy JC, Zavros Y. CD44 variant isoform 9 emerges in response to injury and contributes to the regeneration of the gastric epithelium. *J Pathol* 2017;242:463–475.
40. Khurana SS, Riehl TE, Moore BD, Fassan M, Rugge M, Romero-Gallo J, Noto J, Peek RM Jr, Stenson WF, Mills JC. The hyaluronic acid receptor CD44 coordinates normal and metaplastic gastric epithelial progenitor cell proliferation. *J Biol Chem* 2013;288:16085–16097.
41. Hirata K, Suzuki H, Imaeda H, Matsuzaki J, Tsugawa H, Nagano O, Asakura K, Saya H, Hibi T. CD44 variant 9 expression in primary early gastric cancer as a predictive marker for recurrence. *Br J Cancer* 2013;109:379–386.
42. Leys CM, Nomura S, Rudzinski E, Kaminishi M, Montgomery E, Washington MK, Goldenring JR. Expression of Pdx-1 in human gastric metaplasia and gastric adenocarcinoma. *Hum Pathol* 2006; 37:1162–1168.
43. Saenz JB, Burclaff J, Mills JC. Modeling murine gastric metaplasia through tamoxifen-induced acute parietal cell loss. *Methods Mol Biol* 2016;1422:329–339.
44. Zheng GX, Terry JM, Belgrader P, Ryvkin P, Bent ZW, Wilson R, Ziraldo SB, Wheeler TD, McDermott GP, Zhu J, Gregory MT, Shuga J, Montesclaros L, Underwood JG, Masquelier DA, Nishimura SY, Schnall-Levin M, Wyatt PW, Hindson CM, Bharadwaj R, Wong A, Ness KD, Beppu LW, Deeg HJ, McFarland C, Loeb KR, Valente WJ, Ericson NG, Stevens EA, Radich JP, Mikkelsen TS, Hindson BJ, Bielas JH. Massively parallel digital transcriptional profiling of single cells. *Nat Commun* 2017;8:14049.
45. Wu AR, Neff NF, Kalisky T, Dalerba P, Treutlein B, Rothenberg ME, Mburu FM, Mantalas GL, Sim S, Clarke MF, Quake SR. Quantitative assessment of single-cell RNA-sequencing methods. *Nat Methods* 2014;11:41–46.
46. Ding L, Hayes MM, Photenhauer A, Eaton KA, Li Q, Ocadiz-Ruiz R, Merchant JL. Schlafen 4-expressing myeloid-derived suppressor cells are induced during murine gastric metaplasia. *J Clin Invest* 2016; 126:2867–2880.
47. Juno JA, van Bockel D, Kent SJ, Kelleher AD, Zaunders JJ, Munier CM. Cytotoxic CD4 T cells—friend or foe during viral infection? *Front Immunol* 2017;8:19.
48. Latta M, Mohan K, Issekutz TB. CXCR6 is expressed on T cells in both T helper type 1 (Th1) inflammation and allergen-induced Th2 lung inflammation but is only a weak mediator of chemotaxis. *Immunology* 2007; 121:555–564.
49. Syu LJ, El-Zaatari M, Eaton KA, Liu Z, Tatarbe M, Keeley TM, Pero J, Ferris J, Wilbert D, Kaatz A, Zheng X, Qiao X, Grachtchouk M, Gumucio DL, Merchant JL, Samuelson LC, Dlugosz AA. Transgenic expression of interferon-gamma in mouse stomach leads to inflammation, metaplasia, and dysplasia. *Am J Pathol* 2012; 181:2114–2125.
50. Kang W, Rathinavelu S, Samuelson LC, Merchant JL. Interferon gamma induction of gastric mucous neck cell hypertrophy. *Lab Invest* 2005;85:702–715.
51. Miska J, Lui JB, Toomer KH, Devarajan P, Cai X, Houghton J, Lopez DM, Abreu MT, Wang G, Chen Z. Initiation of inflammatory tumorigenesis by CTLA4 insufficiency due to type 2 cytokines. *J Exp Med* 2018; 215:841–858.
52. Petersen CP, Meyer AR, De Salvo C, Choi E, Schlegel C, Petersen A, Engevik AC, Prasad N, Levy SE, Peebles RS, Pizarro TT, Goldenring JR. A signalling cascade of IL-33 to IL-13 regulates metaplasia in the mouse stomach. *Gut* 2018;67:805–817.
53. Willet SG, Lewis MA, Miao ZF, Liu D, Radyk MD, Cunningham RL, Burclaff J, Sibbel G, Lo HG, Blanc V, Davidson NO, Wang ZN, Mills JC. Regenerative proliferation of differentiated cells by mTORC1-dependent paligenesis. *EMBO J* 2018;37.
54. Li MS, Liu Z, Liu JQ, Zhu X, Liu Z, Bai XF. The Yin and Yang aspects of IL-27 in induction of cancer-specific T-cell responses and immunotherapy. *Immunotherapy* 2015;7:191–200.
55. Nguyen TL, DiPaolo RJ. A new mouse model of inflammation and gastric cancer. *Oncoimmunology* 2013;2: e25911.
56. Nguyen TL, Makhlof NT, Anthony BA, Teague RM, DiPaolo RJ. In vitro induced regulatory T cells are unique from endogenous regulatory T cells and effective at suppressing late stages of ongoing autoimmunity. *PLoS One* 2014;9:e104698.
57. Ramsey VG, Doherty JM, Chen CC, Stappenbeck TS, Konieczny SF, Mills JC. The maturation of mucus-secreting gastric epithelial progenitors into digestive-enzyme secreting zymogenic cells requires Mist1. *Development* 2007;134:211–222.
58. Bockerstett KA, Lewis SA, Wolf KJ, Noto CN, Jackson NM, Ford EL, Ahn TH, DiPaolo RJ. Single-cell transcriptional analyses of spasmolytic polypeptide-expressing metaplasia arising from acute drug injury

- and chronic inflammation in the stomach. *Gut* 2020; 69:1027–1038.
59. Butler A, Hoffman P, Smibert P, Papalexi E, Satija R. Integrating single-cell transcriptomic data across different conditions, technologies, and species. *Nat Biotechnol* 2018;36:411–420.
 60. Ilicic T, Kim JK, Kolodziejczyk AA, Bagger FO, McCarthy DJ, Marioni JC, Teichmann SA. Classification of low quality cells from single-cell RNA-seq data. *Genome Biol* 2016;17:29.
 61. Buettner F, Natarajan KN, Casale FP, Proserpio V, Scialdone A, Theis FJ, Teichmann SA, Marioni JC, Stegle O. Computational analysis of cell-to-cell heterogeneity in single-cell RNA-sequencing data reveals hidden subpopulations of cells. *Nat Biotechnol* 2015; 33:155–160.
 62. Waltman L, van Eck NJ. A smart local moving algorithm for large-scale modularity-based community detection. *Eur Phys J B* 2013;86.
 63. Becht E, McInnes L, Healy J, Dutertre CA, Kwok IWH, Ng LG, Ginhoux F, Newell EW. Dimensionality reduction for visualizing single-cell data using UMAP. *Nat Biotechnol* 2018;37:38–44.

Received March 17, 2020. Accepted April 27, 2020.

Correspondence

Address correspondence to: Richard DiPaolo, PhD, DRC 707, 1100 South Grand Boulevard, Saint Louis, Missouri 63104. e-mail: richard.dipaolo@health.slu.edu; fax: (314) 977-8717.

Acknowledgments

The authors thank Sherri Koehm and Joy Eslick for assistance with flow cytometry; Grant Kolar MD, PhD, Barbara Nagel, and Caroline Murphy from the Saint Louis University Research Microscopy and Histology Core for generation of tissue sections and assistance with confocal microscopy; and the Saint Louis University Comparative Medicine department for assistance in maintaining mouse colonies. The authors also thank John Long, DVM, for

assistance with rIL27 pump implantation procedures. The authors thank Thanh-Long M. Nguyen, PhD, for helping with immunologic and pathologic characterization of the *Ebi3^{-/-}* phenotype, Joseph Burclaff, PhD, for assistance with high-dose tamoxifen studies, Shradha Khurana, PhD, for assistance with semiquantitative analysis of SPFM, and the Advanced Imaging and Tissue Analysis Core of the Washington University Digestive Disease Research Cores Center. The authors also thank Joel Eissenberg, PhD, for critical reading of the manuscript.

CRedit Authorship Contributions

Kevin A. Bockerstett, PhD (Conceptualization: Lead; Data curation: Lead; Formal analysis: Lead; Investigation: Lead; Methodology: Lead; Writing – original draft: Lead); Christine P. Petersen, PhD (Data curation: Supporting; Formal analysis: Supporting); Christine N. Noto, BS (Data curation: Supporting; Formal analysis: Supporting; Writing – review & editing: Supporting); Lindsey M. Kuehm, MS (Formal analysis: Supporting; Investigation: Supporting); Chun Fung Wong, BS (Formal analysis: Supporting; Investigation: Supporting); Eric L. Ford, N/A (Formal analysis: Supporting; Investigation: Supporting); Ryan M Teague, PhD (Conceptualization: Supporting; Resources: Supporting); Jason C. Mills, MD, PhD (Conceptualization: Supporting; Formal analysis: Supporting; Funding acquisition: Supporting; Investigation: Supporting; Writing – review & editing: Supporting); James R. Goldenring, MD, PhD (Conceptualization: Supporting; Funding acquisition: Supporting; Writing – review & editing: Supporting); Richard J DiPaolo, PhD (Conceptualization: Equal; Formal analysis: Equal; Funding acquisition: Lead; Writing – original draft: Equal; Writing – review & editing: Equal).

Conflicts of interest

The authors disclose no conflicts.

Funding

Supported by National Institutes of Health/National Institute of Diabetes and Digestive and Kidney Diseases National Research Service Award predoctoral fellowship F30 DK118873 (K.A.B.); by American Cancer Society grant RSG-12-171-01-LIB and the National Institutes of Health/National Institute of Diabetes and Digestive and Kidney Diseases grant R01 DK110406 (R.J.D. and J.C.M.); a grant from the Digestive Diseases Research Core Center of the Washington University School of Medicine National Institute of Diabetes and Digestive and Kidney Diseases P30DK52574, by the American Gastroenterological Association Funderburg Research Award (R.J.D.); by VA Merit Review 1I01BX000930 and National Institutes of Health grant DK101332 (J.R.G.); by a National Institutes of Health NRSA predoctoral fellowship F31 DK104600 (C.P.P.); and by the Alvin J. Siteman Cancer Center/Barnes-Jewish Hospital Foundation Cancer Frontier Fund grant P30 CA091842 and the National Institutes of Health/ National Institute of Diabetes and Digestive and Kidney Diseases grants R01 DK094989, R01 DK105129, and DK P30DK052574 (J.C.M.).